US 20140010700A1

(19) **United States**

(12) **Patent Application Publication** (10) **Pub. No.: US 2014/0010700 A1**

Pandey (43) **Pub. Date: Jan. 9, 2014**

(54) **DIRECT EXTRUSION OF SHAPES WITH L12 ALUMINUM ALLOYS**

(71) Applicant: **United Technologies Corporation**, Hartford, CT (US)

(72) Inventor: **Awadh B. Pandey**, Jupiter, FL (US)

(21) Appl. No.: **13/925,988**

(22) Filed: **Jun. 25, 2013**

Related U.S. Application Data

(62) Division of application No. 12/560,000, filed on Sep. 15, 2009, now abandoned.

Publication Classification

(51) **Int. Cl.**

B22F 3/20 (2006.01)

(52) **U.S. Cl.**

CPC ***B22F 3/20*** (2013.01)

USPC **419/12**; 419/23; 419/19; 419/17; 419/13

(57) **ABSTRACT**

A method for producing a high strength aluminum alloy brackets, cases, tubes, ducts, beams, spars and other parts containing $L1_2$ dispersoids from an aluminum alloy powder containing the $L1_2$ dispersoids. The powder is consolidated into a billet having a density of about 100 percent. The billet is extruded using an extrusion die shaped to produce the component.

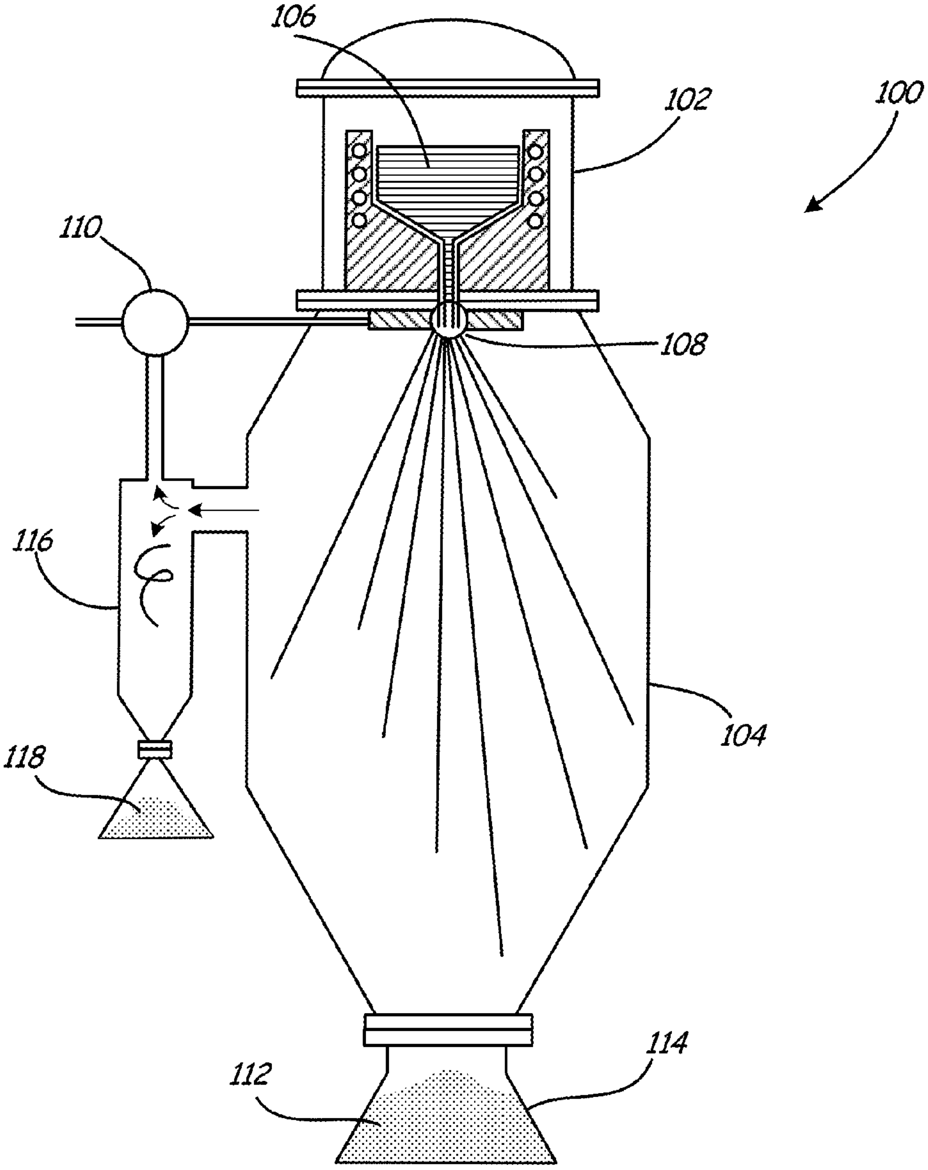

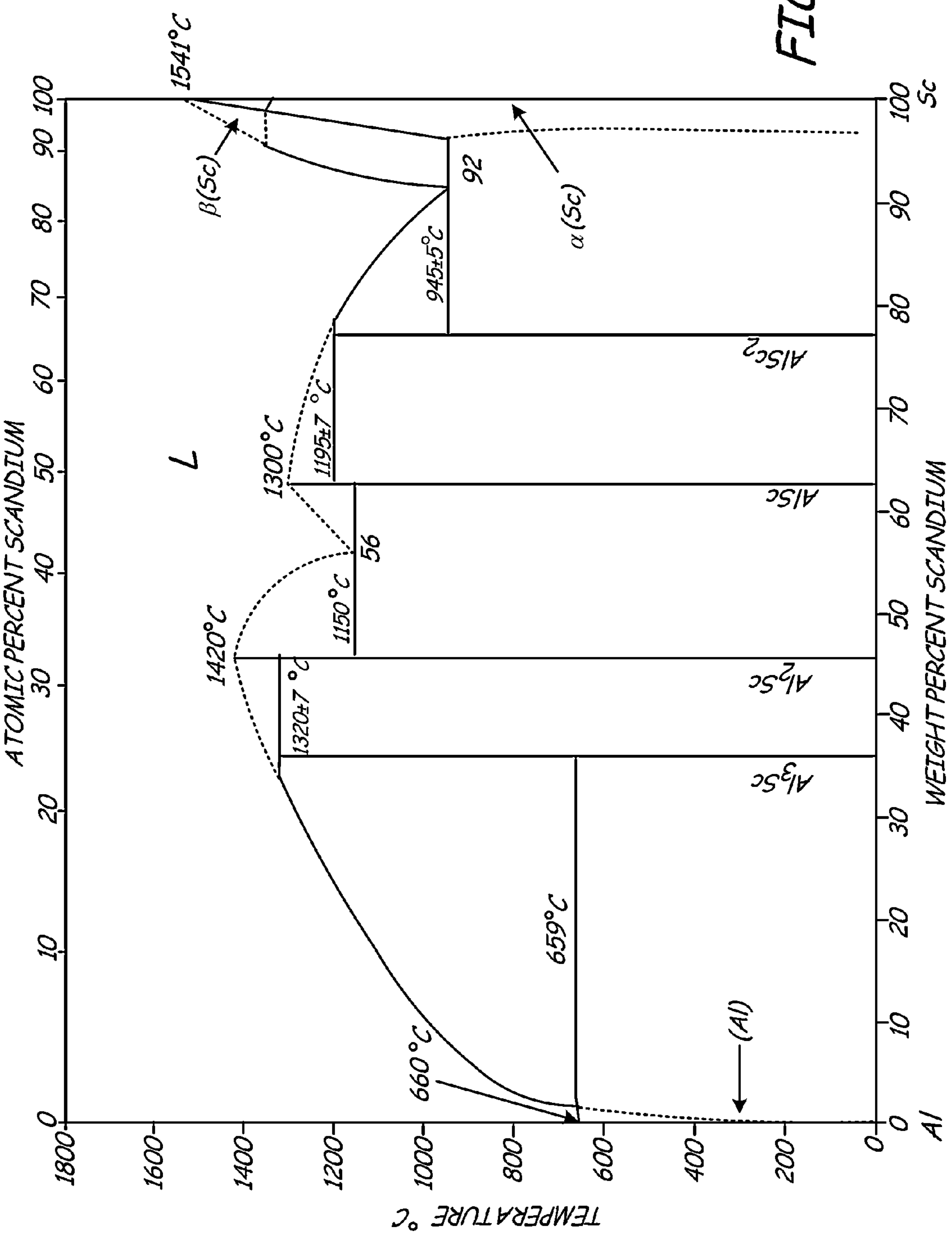
ATOMIC PERCENT SCANDIUM
0
10
20
30
40
50
60
70
80
90
100
WEIGHT PERCENT SCANDIUM
0
10
20
30
40
50
60
70
80
90
100
Al
Sc
TEMPERATURE °C
1800
1600
1400
1200
1000
800
600
400
200
0
1541°C
β(Sc)
α(Sc)
92
945±5°C
L
1300°C
1195±7 °C
56
1150°C
1420°C
1320±7 °C
659°C
660°C
(Al)
AlSc₂
AlSc
Al₂Sc
Al₃Sc

FIG. 1

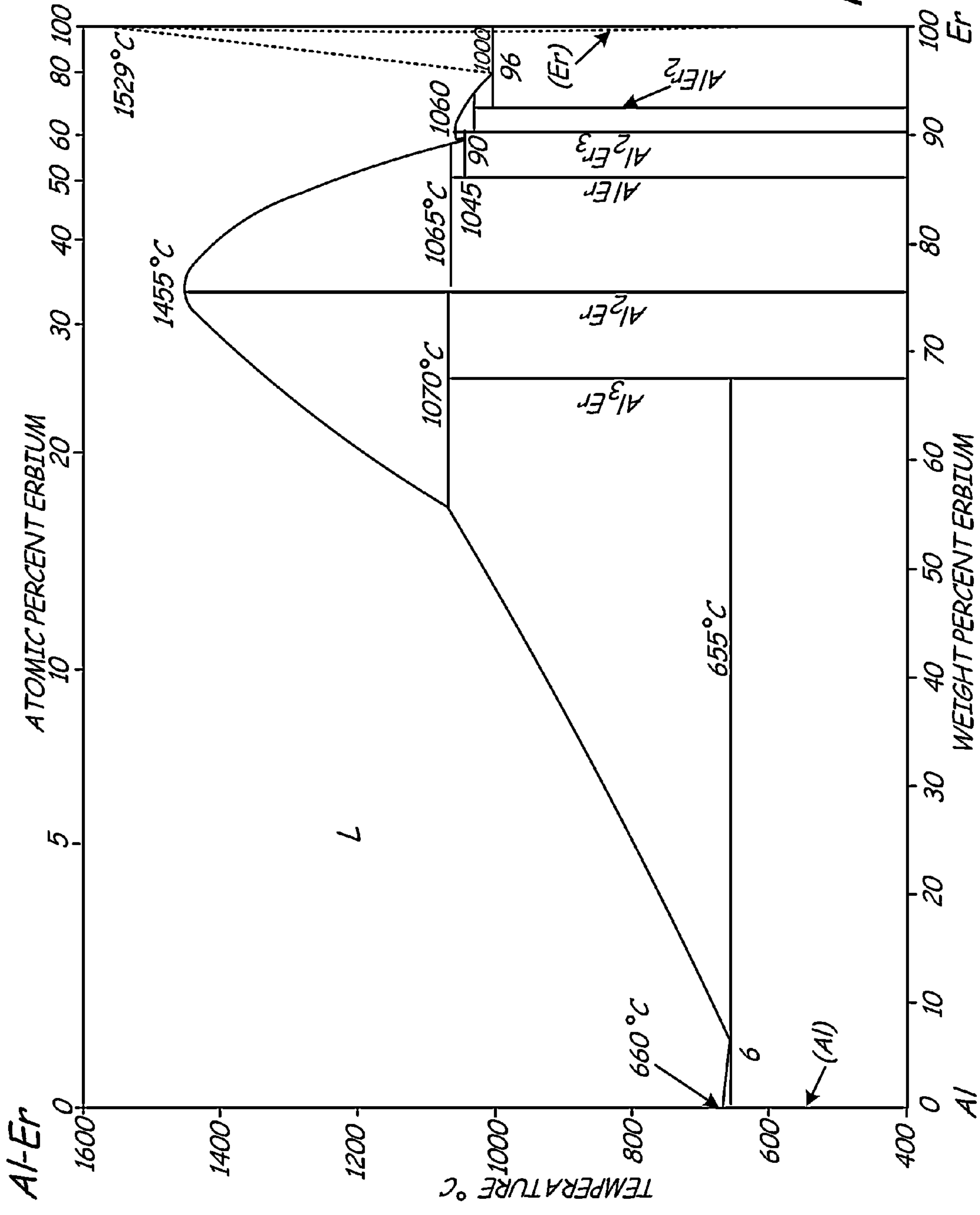
Al-Er
ATOMIC PERCENT ERBIUM
0
5
10
20
30
40
50
60
80
100
TEMPERATURE °C
1600
1400
1200
1000
800
600
400
WEIGHT PERCENT ERBIUM
Al
0
10
20
30
40
50
60
70
80
90
100
Er
L
660°C
6
(Al)
655°C
1070°C
1455°C
1065°C
1045
90
1060
1000
96
1529°C
(Er)
Al_3Er
Al_2Er
AlEr
Al_2Er_3
$AlEr_2$

FIG. 2

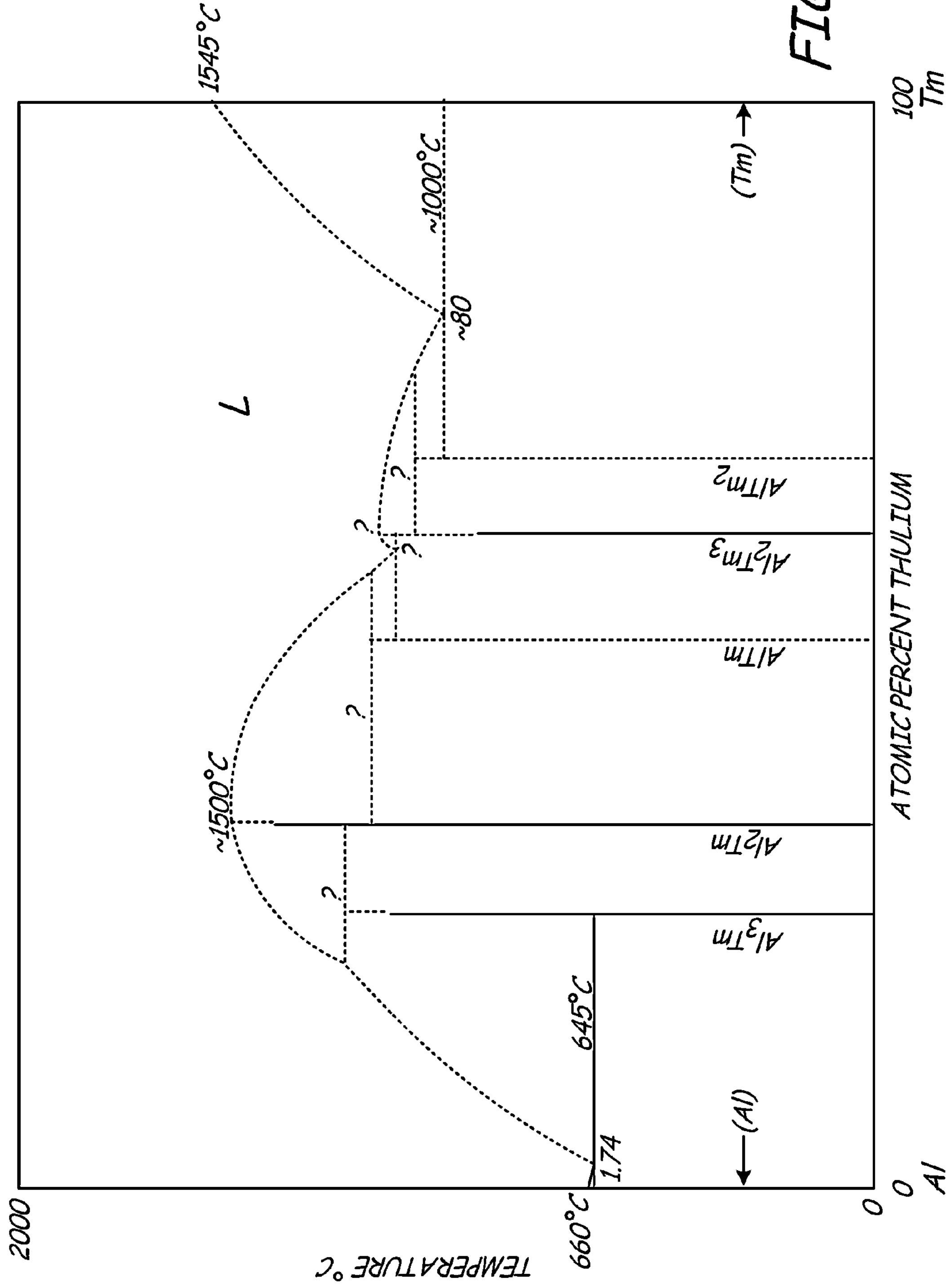
2000
660°C
0
TEMPERATURE °C
1.74
645°C
(Al)
~1500°C
?
?
?
?
?
?
L
~80
~1000°C
1545°C
(Tm)
Al_3Tm
Al_2Tm
AlTm
Al_2Tm_3
$AlTm_2$
0
Al
100
Tm
ATOMIC PERCENT THULIUM

FIG. 3

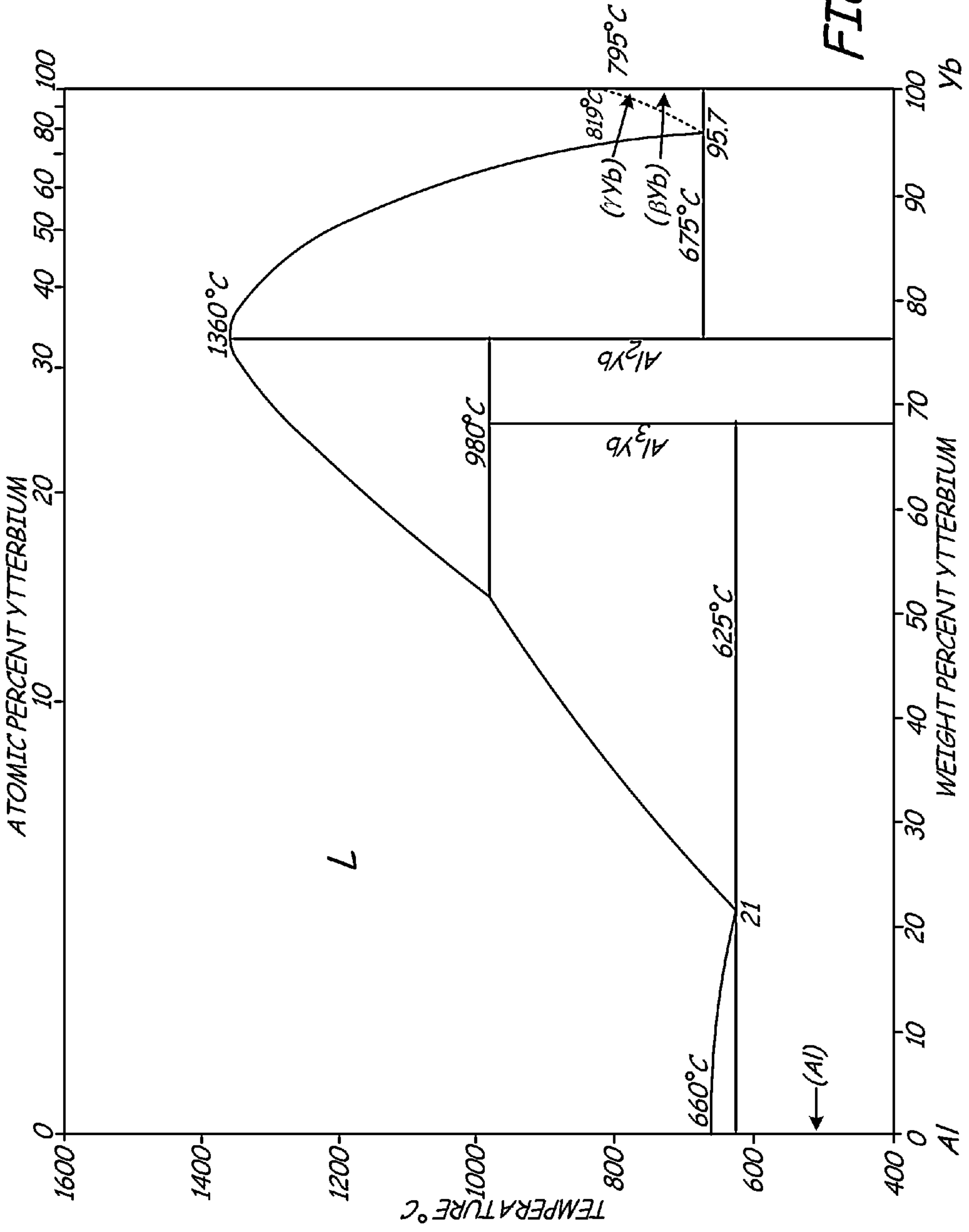
ATOMIC PERCENT YTTERBIUM
0
10
20
30
40
50
60
70
80
100
TEMPERATURE °C
1600
1400
1200
1000
800
600
400
L
660°C
21
625°C
980°C
1360°C
Al_3Yb
Al_2Yb
675°C
(βYb)
(γYb)
819°C
795°C
95.7
(Al)
WEIGHT PERCENT YTTERBIUM
Al
0
10
20
30
40
50
60
70
80
90
100
Yb

FIG. 4

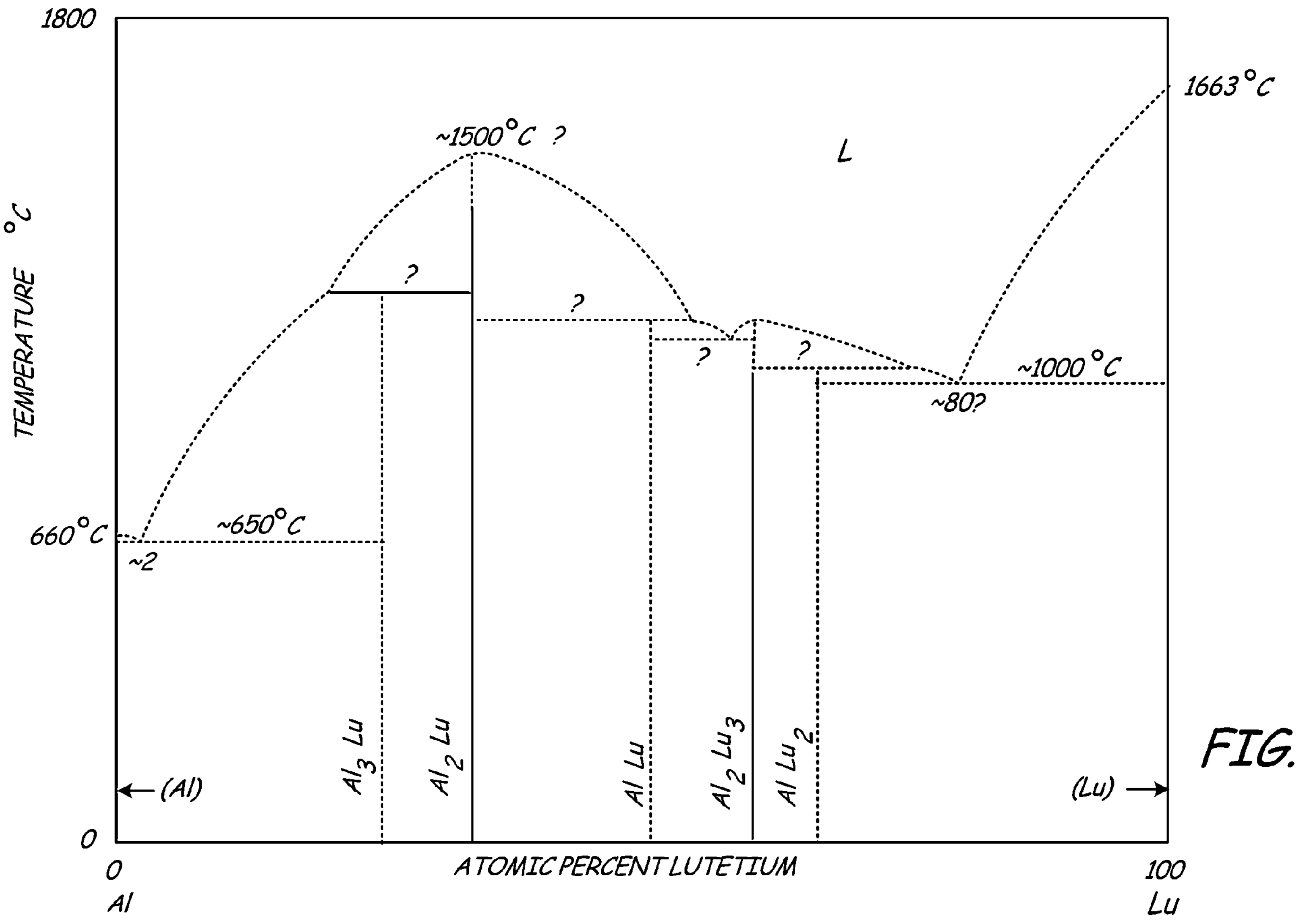

1800
660°C
0
TEMPERATURE °C
~2
~650°C
~1500°C ?
?
?
?
?
L
1663°C
~1000°C
~80?
$Al_3 Lu$
$Al_2 Lu$
Al Lu
$Al_2 Lu_3$
$Al Lu_2$
← (Al)
(Lu) →
0
Al
ATOMIC PERCENT LUTETIUM
100
Lu

FIG. 5

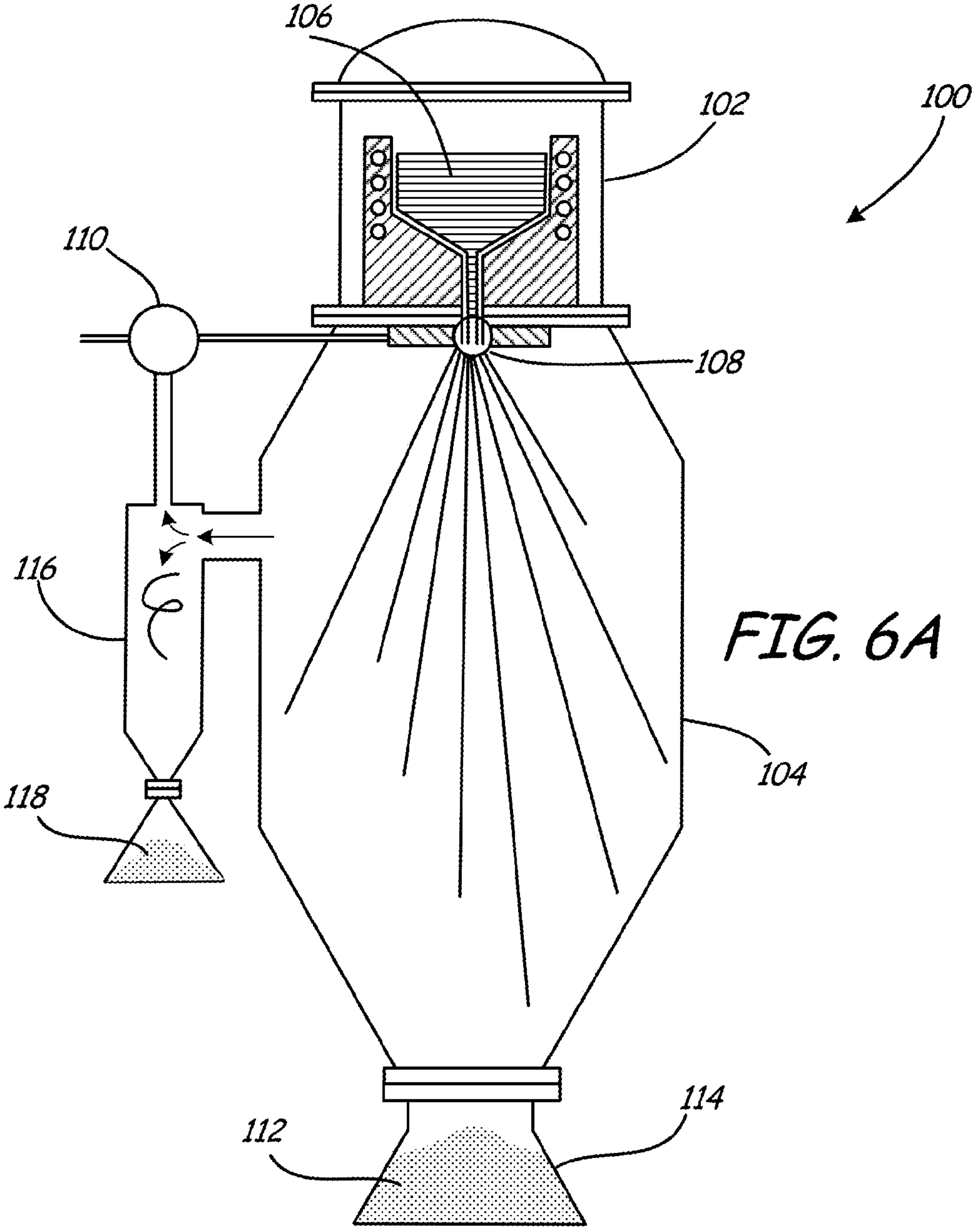

FIG. 6A

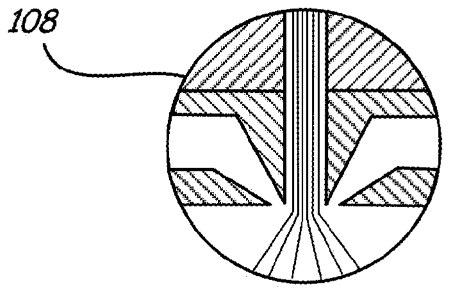

FIG. 6B

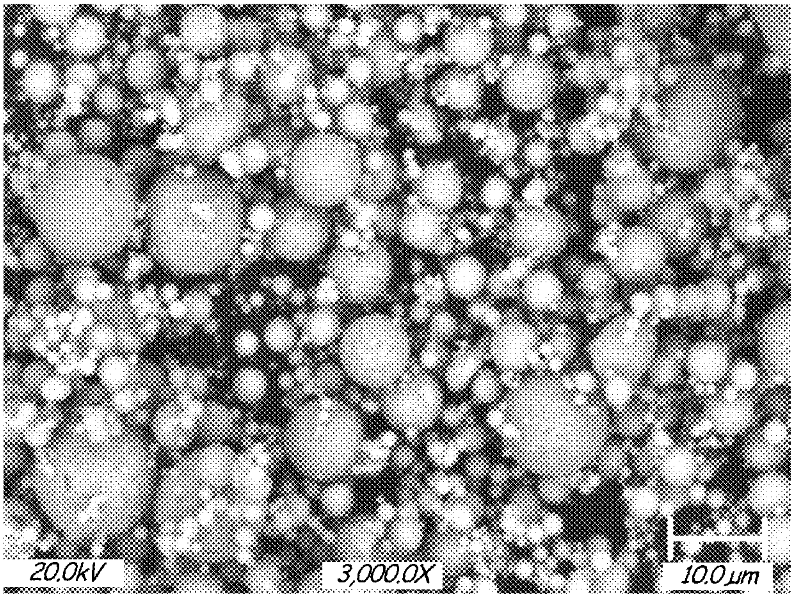

FIG. 7A

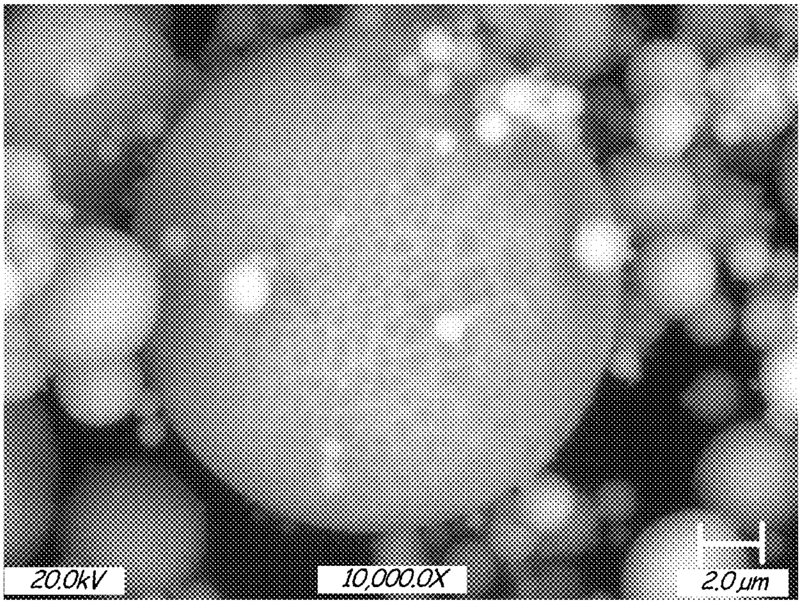

FIG. 7B

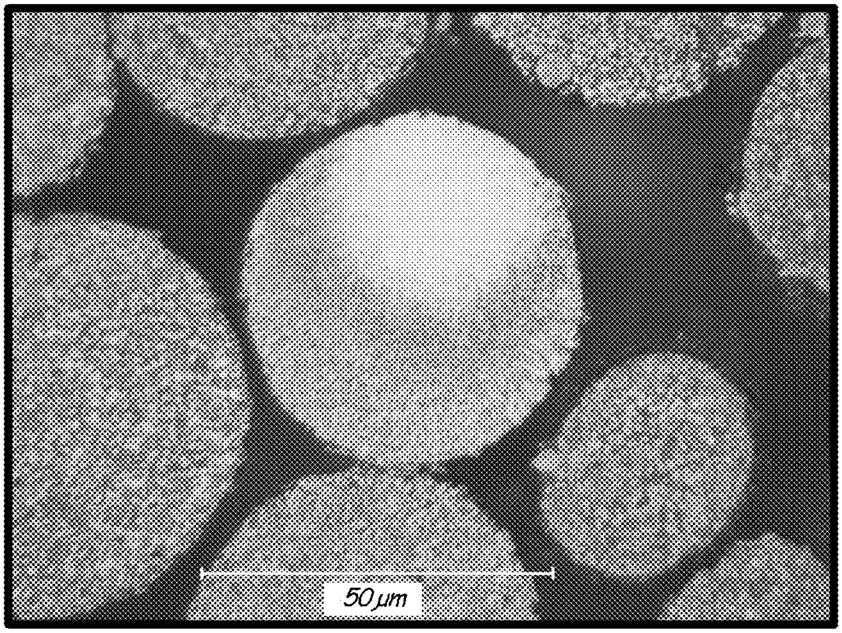

FIG. 8A

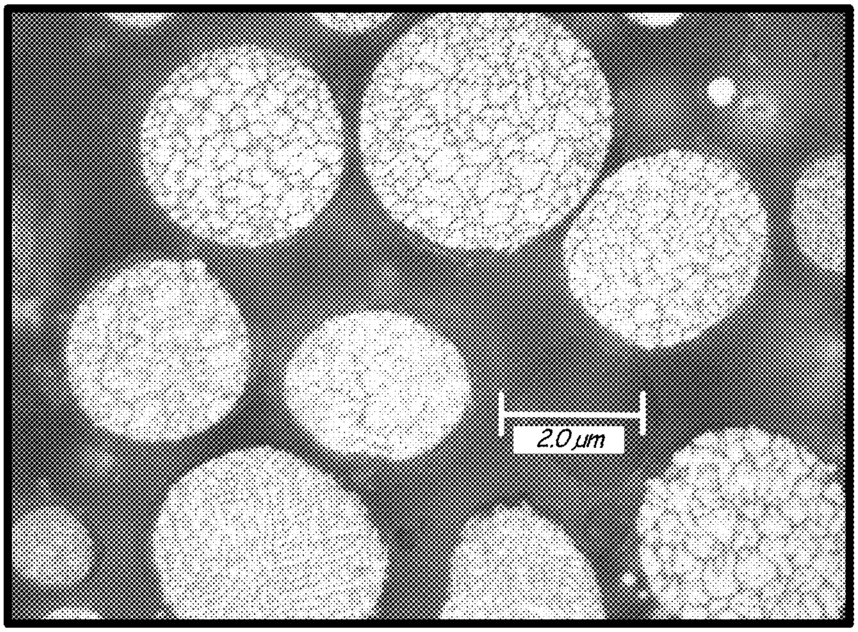

FIG. 8B

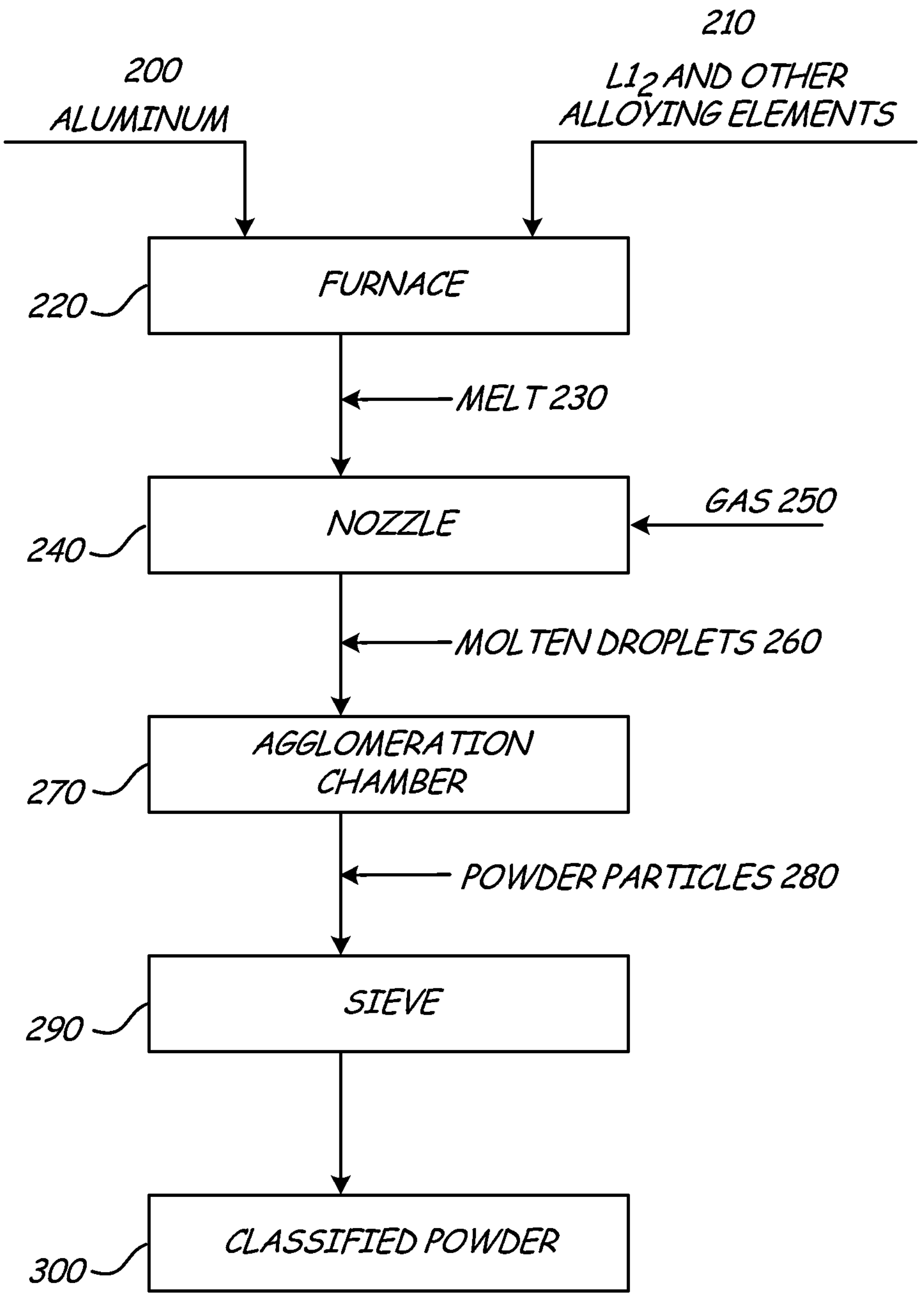
200
ALUMINUM
210
L1₂ AND OTHER ALLOYING ELEMENTS
220
FURNACE
MELT 230
240
NOZZLE
GAS 250
MOLTEN DROPLETS 260
270
AGGLOMERATION CHAMBER
POWDER PARTICLES 280
290
SIEVE
300
CLASSIFIED POWDER

FIG. 9

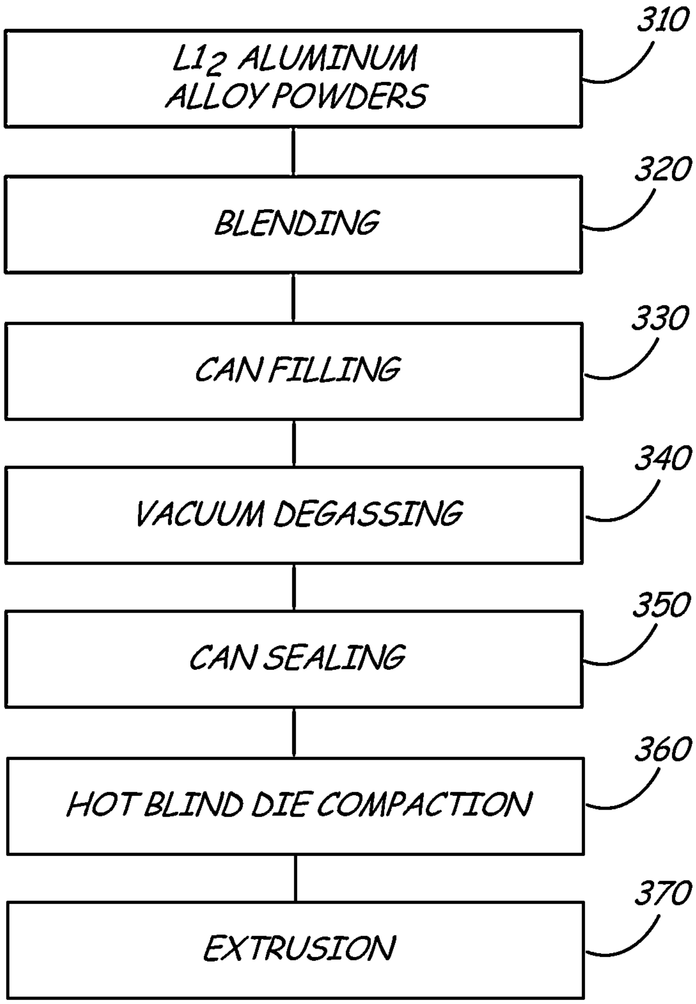
L1$_2$ ALUMINUM ALLOY POWDERS
310
BLENDING
320
CAN FILLING
330
VACUUM DEGASSING
340
CAN SEALING
350
HOT BLIND DIE COMPACTION
360
EXTRUSION
370

FIG. 10

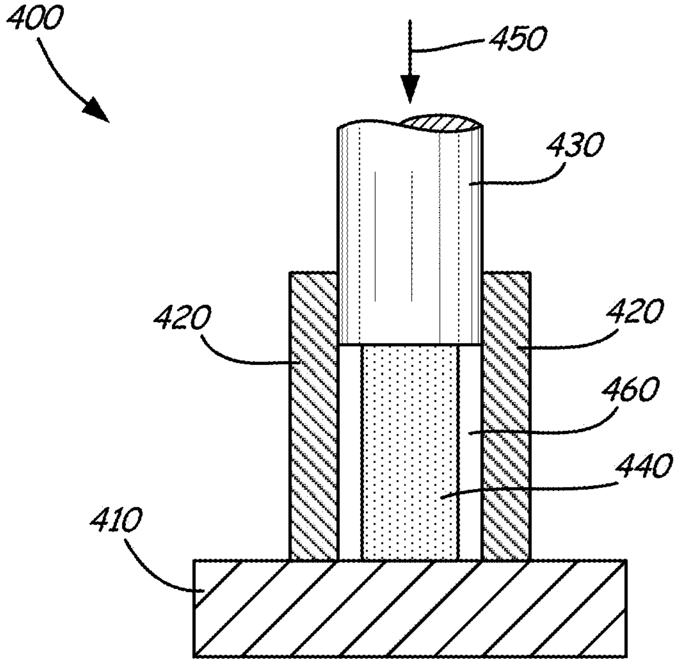

FIG. 11A

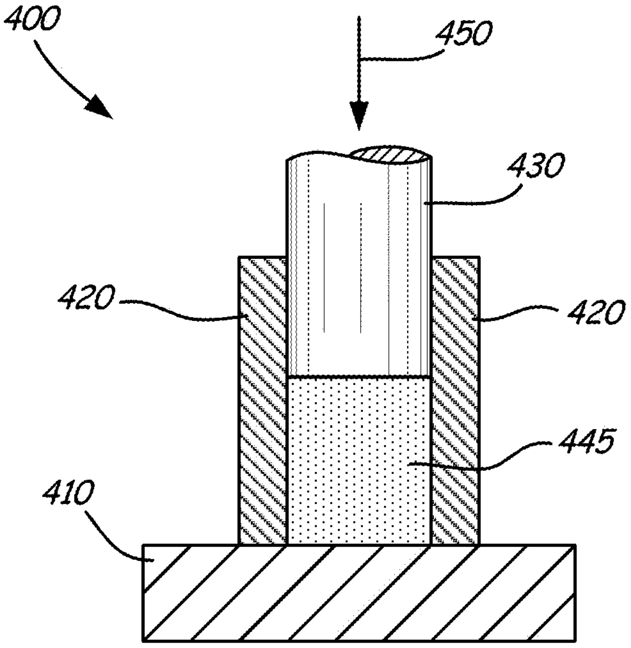

FIG. 11B

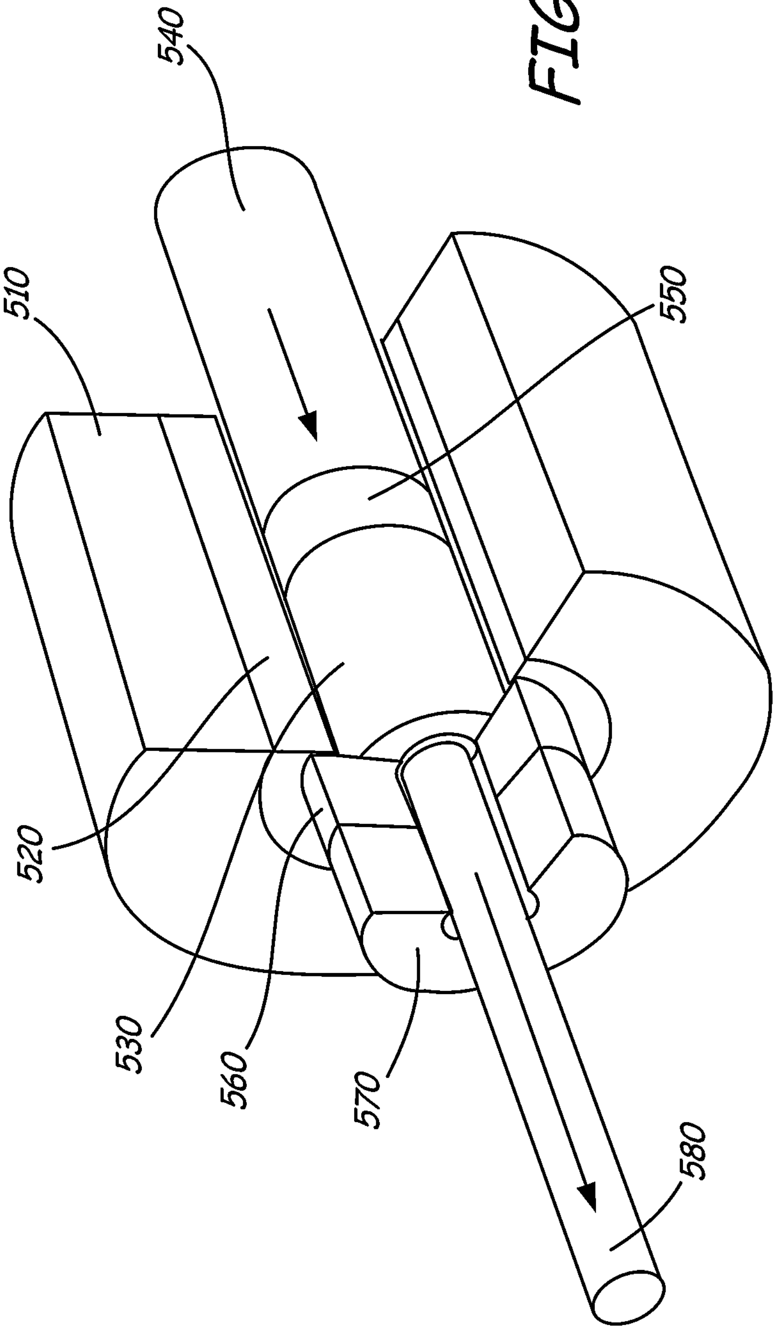

FIG. 12

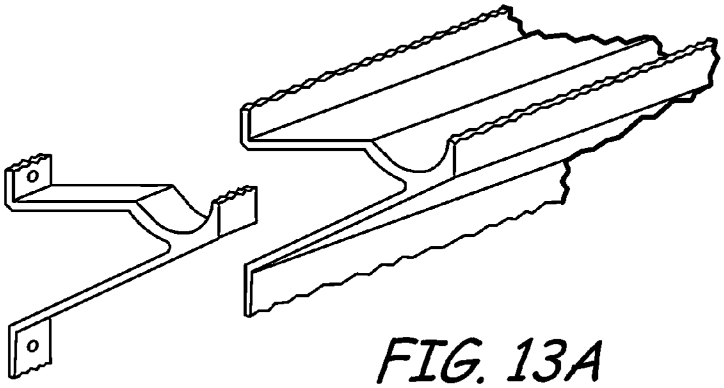

FIG. 13A

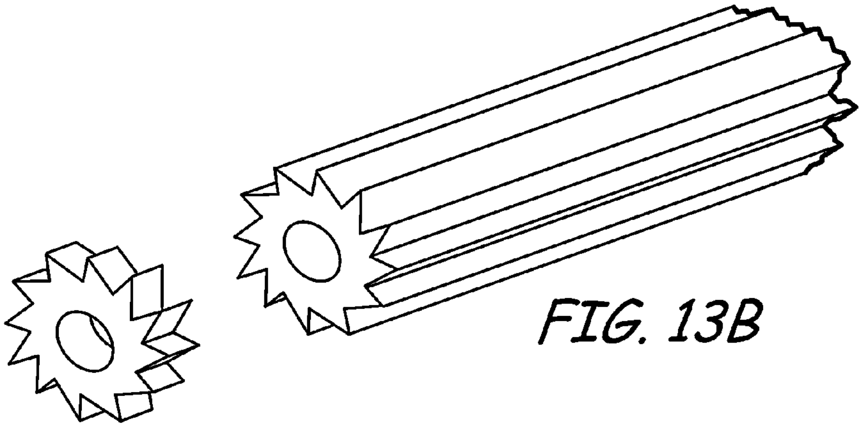

FIG. 13B

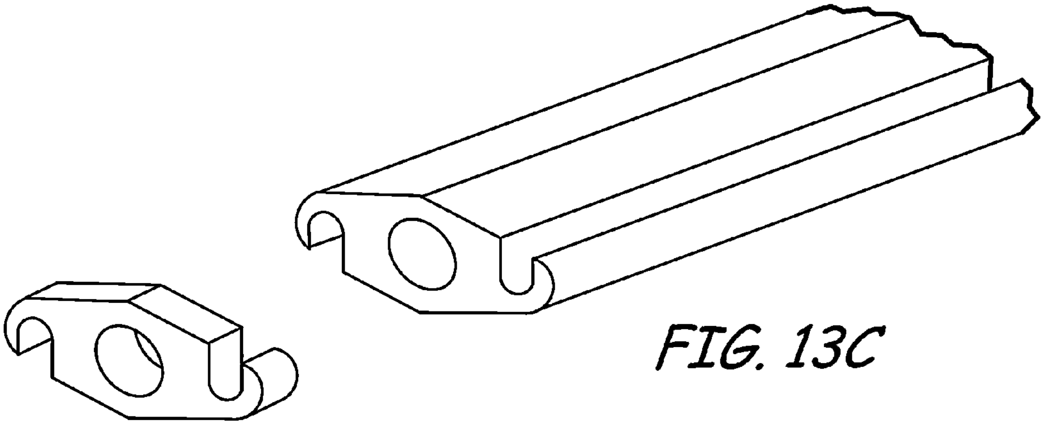

FIG. 13C

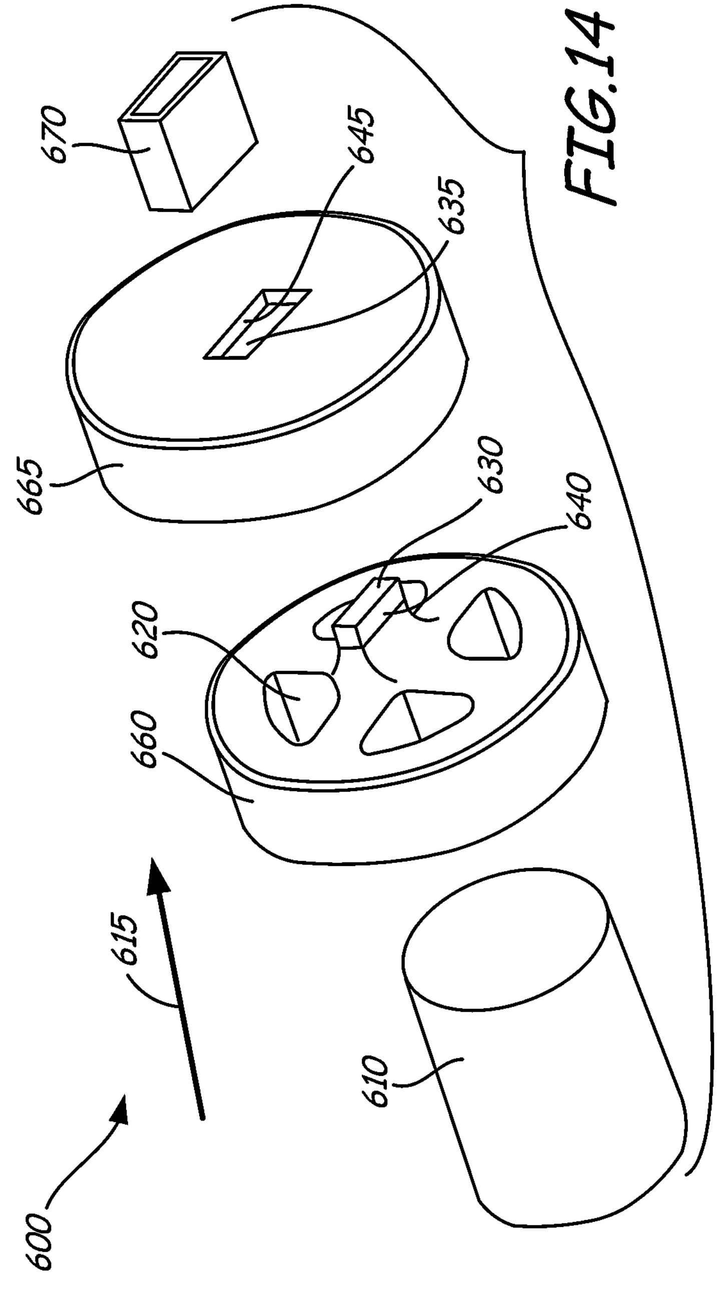

FIG.14

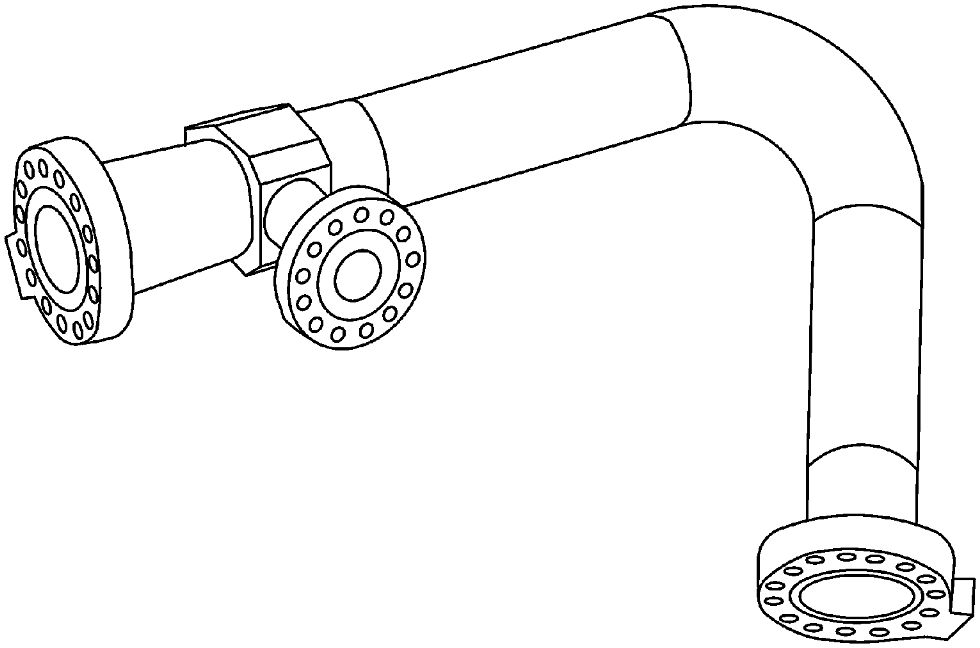

FIG. 15

DIRECT EXTRUSION OF SHAPES WITH L12 ALUMINUM ALLOYS

CROSS-REFERENCE TO RELATED APPLICATION(S)

[0001] This application is a divisional of application Ser. No. 12/560,000, filed Sep. 15, 2009; which is related to the following co-pending applications that were filed on Dec. 9, 2008 herewith and are assigned to the same assignee: CONVERSION PROCESS FOR HEAT TREATABLE $L1_2$ ALUMINUM ALLOYS, Ser. No. 12/316,020; A METHOD FOR FORMING HIGH STRENGTH ALUMINUM ALLOYS CONTAINING $L1_2$ INTERMETALLIC DISPERSOIDS, Ser. No. 12/316,046; and A METHOD FOR PRODUCING HIGH STRENGTH ALUMINUM ALLOY POWDER CONTAINING $L1_2$ INTERMETALLIC DISPERSOIDS, Ser. No. 12/316,047. All references are incorporated herein.

[0002] This application is also related to the following co-pending applications that were filed on Apr. 18, 2008, and are assigned to the same assignee: $L1_2$ ALUMINUM ALLOYS WITH BIMODAL AND TRIMODAL DISTRIBUTION, Ser. No. 12/148,395; DISPERSION STRENGTHENED $L1_2$ ALUMINUM ALLOYS, Ser. No. 12/148,432; HEAT TREATABLE $L1_2$ ALUMINUM ALLOYS, Ser. No. 12/148,383; HIGH STRENGTH $L1_2$ ALUMINUM ALLOYS, Ser. No. 12/148,394; HIGH STRENGTH $L1_2$ ALUMINUM ALLOYS, Ser. No. 12/148,382; HEAT TREATABLE $L1_2$ ALUMINUM ALLOYS, Ser. No. 12/148,396; HIGH STRENGTH $L1_2$ ALUMINUM ALLOYS, Ser. No. 12/148,387; HIGH STRENGTH ALUMINUM ALLOYS WITH $L1_2$ PRECIPITATES, Ser. No. 12/148,426; HIGH STRENGTH $L1_2$ ALUMINUM ALLOYS, Ser. No. 12/148,459; and $L1_2$ STRENGTHENED AMORPHOUS ALUMINUM ALLOYS, Ser. No. 12/148,458.

BACKGROUND

[0003] The present invention relates generally to aluminum alloys and more specifically to a method for forming high strength aluminum ally powder having $L1_2$ dispersoids therein into aluminum parts such as brackets, cases and other components of turbine engines as well as other products fabricated from aluminum alloys.

[0004] The combination of high strength, ductility, and fracture toughness, as well as low density, make aluminum alloys natural candidates for as variety of applications. Because of its low weight high strength, ductility and fracture toughness, aluminum alloys are of interest in the manufacture and use for many applications.

[0005] The development of aluminum alloys with improved elevated temperature mechanical properties is a continuing process. Some attempts have included aluminum-iron and aluminum-chromium based alloys such as Al—Fe—Ce, Al—Fe—V—Si, Al—Fe—Ce—W, and Al—Cr—Zr—Mn that contain incoherent dispersoids. These alloys, however, also lose strength at elevated temperatures due to particle coarsening. In addition, these alloys exhibit ductility and fracture toughness values lower than other commercially available aluminum alloys.

[0006] Other attempts have included the development of mechanically alloyed Al—Mg and Al—Ti alloys containing ceramic dispersoids. These alloys exhibit improved high temperature strength due to the particle dispersion, but the ductility and fracture toughness are not improved.

[0007] U.S. Pat. No. 6,248,453 discloses aluminum alloys strengthened by dispersed Al_3X $L1_2$ intermetallic phases where X is selected from the group consisting of Sc, Er, Lu, Yb, Tm, and Lu. The Al_3X particles are coherent with the aluminum alloy matrix and are resistant to coarsening at elevated temperatures. The improved mechanical properties of the disclosed dispersion strengthened $L1_2$ aluminum alloys are stable up to 572° F. (300° C.). U.S. Patent Application Publication No. 2006/0269437 A1 discloses a high strength aluminum alloy that contains scandium and other elements that is strengthened by $L1_2$ dispersoids.

[0008] $L1_2$ strengthened aluminum alloys have high strength and improved fatigue properties compared to commercial aluminum alloys. Fine grain size results in improved mechanical properties of materials. Hall-Petch strengthening has been known for decades where strength increases as grain size decreases. An optimum grain size for optimum strength is in the nano range of about 30 to 100 nm. These alloys also have higher ductility.

SUMMARY

[0009] The present invention is a method for consolidating aluminum alloy powders into useful components such as brackets, cases and other components having improved strength and fracture toughness. In embodiments, powders include an aluminum alloy having coherent $L1_2$ Al_3X dispersoids where X is at least one first element selected from scandium, erbium, thulium, ytterbium, and lutetium, and at least one second element selected from gadolinium, yttrium, zirconium, titanium, hafnium, and niobium. The balance is substantially aluminum containing at least one alloying element selected from silicon, magnesium, manganese, lithium, copper, zinc, and nickel.

[0010] The aluminum alloy components and parts are formed by direct extrusion of consolidated billets using a die with the required component shape. Extrusion of these alloys produces considerable improvement in mechanical properties, especially ductility compared to the consolidated billet. Extrusion parameters include billet temperature, billet soak time, extrusion rate, extrusion ratio and die temperature.

BRIEF DESCRIPTION OF THE DRAWINGS

[0011] FIG. **1** is an aluminum scandium phase diagram.

[0012] FIG. **2** is an aluminum erbium phase diagram.

[0013] FIG. **3** is an aluminum thulium phase diagram.

[0014] FIG. **4** is an aluminum ytterbium phase diagram.

[0015] FIG. **5** is an aluminum lutetium phase diagram.

[0016] FIG. **6**A is a schematic diagram of a vertical gas atomizer.

[0017] FIG. **6**B is a close up view of nozzle **108** in FIG. **6**A.

[0018] FIGS. **7**A and **7**B are SEM photos of the inventive aluminum alloy powder.

[0019] FIGS. **8**A and **8**B are optical micrographs showing the microstructure of gas atomized $L1_2$ aluminum alloy powder.

[0020] FIG. **9** is a diagram showing the steps of the gas atomization process.

[0021] FIG. **10** is a diagram showing the processing steps to consolidate the $L1_2$ aluminum alloy powder.

[0022] FIG. **11**A-B are schematic diagrams of blind die compaction.

[0023] FIG. **12** is a schematic diagram of a direct extrusion process.

[0024] FIG. **13** A-C are extrusions and examples of products made by sectioning off extrusions.

[0025] FIG. **14** is a schematic of a hollow extrusion die.

[0026] FIG. **15** is a photograph of duct produced for a rocket engine.

DETAILED DESCRIPTION

1. $L1_2$ Aluminum Alloys

[0027] Alloy powders of this invention are formed from aluminum based alloys with high strength and fracture toughness for applications at temperatures from about −420° F. (−251° C.) up to about 650° F. (343° C.). The aluminum alloy comprises a solid solution of aluminum and at least one element selected from silicon, magnesium, manganese, lithium, copper, zinc, and nickel strengthened by $L1_2$ Al_3X coherent precipitates where X is at least one first element selected from scandium, erbium, thulium, ytterbium, and lutetium, and at least one second element selected from gadolinium, yttrium, zirconium, titanium, hafnium, and niobium.

[0028] The binary aluminum magnesium system is a simple eutectic at 36 weight percent magnesium and 842° F. (450° C.). There is complete solubility of magnesium and aluminum in the rapidly solidified inventive alloys discussed herein

[0029] The binary aluminum silicon system is a simple eutectic at 12.6 weight percent silicon and 1070.6° F. (577° C.). There is complete solubility of silicon and aluminum in the rapidly solidified inventive alloys discussed herein.

[0030] The binary aluminum manganese system is a simple eutectic at about 2 weight percent manganese and 1216.4° F. (658° C.). There is complete solubility of manganese and aluminum in the rapidly solidified inventive alloys discussed herein.

[0031] The binary aluminum lithium system is a simple eutectic at 8 weight percent lithium and 1105° (596° C.). The equilibrium solubility of 4 weight percent lithium can be extended significantly by rapid solidification techniques. There is complete solubility of lithium in the rapid solidified inventive alloys discussed herein.

[0032] The binary aluminum copper system is a simple eutectic at 32 weight percent copper and 1018° F. (548° C.). There is complete solubility of copper in the rapidly solidified inventive alloys discussed herein.

[0033] The aluminum zinc binary system is a eutectic alloy system involving a monotectoid reaction and a miscibility gap in the solid state. There is a eutectic reaction at 94 weight percent zinc and 718° F. (381° C.). Zinc has maximum solid solubility of 83.1 weight percent in aluminum at 717.8° F. (381° C.), which can be extended by rapid solidification processes. Decomposition of the supersaturated solid solution of zinc in aluminum gives rise to spherical and ellipsoidal GP zones, which are coherent with the matrix and act to strengthen the alloy.

[0034] The aluminum nickel binary system is a simple eutectic at 5.7 weight percent nickel and 1183.8° F. (639.9° C.). There is little solubility of nickel in aluminum. However, the solubility can be extended significantly by utilizing rapid solidification processes. The equilibrium phase in the aluminum nickel eutectic system is $L1_2$ intermetallic Al_3Ni.

[0035] In the aluminum based alloys disclosed herein, scandium, erbium, thulium, ytterbium, and lutetium are potent strengtheners that have low diffusivity and low solubility in aluminum. All these elements form equilibrium Al_3X intermetallic dispersoids where X is at least one of scandium, erbium, thulium, ytterbium, and lutetium, that have an $L1_2$ structure that is an ordered face centered cubic structure with the X atoms located at the corners and aluminum atoms located on the cube faces of the unit cell.

[0036] Scandium forms Al_3Sc dispersoids that are fine and coherent with the aluminum matrix. Lattice parameters of aluminum and Al_3Sc are very close (0.405 nm and 0.410 nm respectively), indicating that there is minimal or no driving force for causing growth of the Al_3Sc dispersoids. This low interfacial energy makes the Al_3Sc dispersoids thermally stable and resistant to coarsening up to temperatures as high as about 842° F. (450° C.). Additions of magnesium in aluminum increase the lattice parameter of the aluminum matrix, and decrease the lattice parameter mismatch further increasing the resistance of the Al_3Sc to coarsening. Additions of zinc, copper, lithium, silicon, manganese and nickel provide solid solution and precipitation strengthening in the aluminum alloys. These Al_3Sc dispersoids are made stronger and more resistant to coarsening at elevated temperatures by adding suitable alloying elements such as gadolinium, yttrium, zirconium, titanium, hafnium, niobium, or combinations thereof, that enter Al_3Sc in solution.

[0037] Erbium forms Al_3Er dispersoids in the aluminum matrix that are fine and coherent with the aluminum matrix. The lattice parameters of aluminum and Al_3Er are close (0.405 nm and 0.417 nm respectively), indicating there is minimal driving force for causing growth of the Al_3Er dispersoids. This low interfacial energy makes the Al_3Er dispersoids thermally stable and resistant to coarsening up to temperatures as high as about 842° F. (450° C.). Additions of magnesium in aluminum increase the lattice parameter of the aluminum matrix, and decrease the lattice parameter mismatch further increasing the resistance of the Al_3Er to coarsening. Additions of zinc, copper, lithium, silicon, manganese and nickel provide solid solution and precipitation strengthening in the aluminum alloys. These Al_3Er dispersoids are made stronger and more resistant to coarsening at elevated temperatures by adding suitable alloying elements such as gadolinium, yttrium, zirconium, titanium, hafnium, niobium, or combinations thereof that enter Al_3Er in solution.

[0038] Thulium forms metastable Al_3Tm dispersoids in the aluminum matrix that are fine and coherent with the aluminum matrix. The lattice parameters of aluminum and Al_3Tm are close (0.405 nm and 0.420 nm respectively), indicating there is minimal driving force for causing growth of the Al_3Tm dispersoids. This low interfacial energy makes the Al_3Tm dispersoids thermally stable and resistant to coarsening up to temperatures as high as about 842° F. (450° C.). Additions of magnesium in aluminum increase the lattice parameter of the aluminum matrix, and decrease the lattice parameter mismatch further increasing the resistance of the Al_3Tm to coarsening. Additions of zinc, copper, lithium, silicon, manganese and nickel provide solid solution and precipitation strengthening in the aluminum alloys. These Al_3Tm dispersoids are made stronger and more resistant to coarsening at elevated temperatures by adding suitable alloying elements such as gadolinium, yttrium, zirconium, titanium, hafnium, niobium, or combinations thereof that enter Al_3Tm in solution.

[0039] Ytterbium forms Al_3Yb dispersoids in the aluminum matrix that are fine and coherent with the aluminum matrix. The lattice parameters of Al and Al_3Yb are close (0.405 nm and 0.420 nm respectively), indicating there is minimal driving force for causing growth of the Al_3Yb dispersoids. This low interfacial energy makes the Al_3Yb dispersoids thermally stable and resistant to coarsening up to temperatures as high as about 842° F. (450° C.). Additions of magnesium in aluminum increase the lattice parameter of the aluminum matrix, and decrease the lattice parameter mismatch further increasing the resistance of the Al_3Yb to coarsening. Additions of zinc, copper, lithium, silicon, manganese and nickel provide solid solution and precipitation strengthening in the aluminum alloys. These Al_3Yb dispersoids are made stronger and more resistant to coarsening at elevated temperatures by adding suitable alloying elements such as gadolinium, yttrium, zirconium, titanium, hafnium, niobium, or combinations thereof that enter Al_3Yb in solution.

[0040] Lutetium forms Al_3Lu dispersoids in the aluminum matrix that are fine and coherent with the aluminum matrix. The lattice parameters of Al and Al_3Lu are close (0.405 nm and 0.419 nm respectively), indicating there is minimal driving force for causing growth of the Al_3Lu dispersoids. This low interfacial energy makes the Al_3Lu dispersoids thermally stable and resistant to coarsening up to temperatures as high as about 842° F. (450° C.). Additions of magnesium in aluminum increase the lattice parameter of the aluminum matrix, and decrease the lattice parameter mismatch further increasing the resistance of the Al_3Lu to coarsening. Additions of zinc, copper, lithium, silicon, manganese and nickel provide solid solution and precipitation strengthening in the aluminum alloys. These Al_3Lu dispersoids are made stronger and more resistant to coarsening at elevated temperatures by adding suitable alloying elements such as gadolinium, yttrium, zirconium, titanium, hafnium, niobium, or mixtures thereof that enter Al_3Lu in solution.

[0041] Gadolinium forms metastable Al_3Gd dispersoids in the aluminum matrix that are stable up to temperatures as high as about 842° F. (450° C.) due to their low diffusivity in aluminum. The Al_3Gd dispersoids have a $D0_{19}$ structure in the equilibrium condition. Despite its large atomic size, gadolinium has fairly high solubility in the Al_3X intermetallic dispersoids (where X is scandium, erbium, thulium, ytterbium or lutetium). Gadolinium can substitute for the X atoms in Al_3X intermetallic, thereby forming an ordered $L1_2$ phase which results in improved thermal and structural stability.

[0042] Yttrium forms metastable Al_3Y dispersoids in the aluminum matrix that have an $L1_2$ structure in the metastable condition and a $D0_{19}$ structure in the equilibrium condition. The metastable Al_3Y dispersoids have a low diffusion coefficient, which makes them thermally stable and highly resistant to coarsening. Yttrium has a high solubility in the Al_3X intermetallic dispersoids allowing large amounts of yttrium to substitute for X in the Al_3X $L1_2$ dispersoids, which results in improved thermal and structural stability.

[0043] Zirconium forms Al_3Zr dispersoids in the aluminum matrix that have an $L1_2$ structure in the metastable condition and $D0_{23}$ structure in the equilibrium condition. The metastable Al_3Zr dispersoids have a low diffusion coefficient, which makes them thermally stable and highly resistant to coarsening. Zirconium has a high solubility in the Al_3X dispersoids allowing large amounts of zirconium to substitute for X in the Al_3X dispersoids, which results in improved thermal and structural stability.

[0044] Titanium forms Al_3Ti dispersoids in the aluminum matrix that have an $L1_2$ structure in the metastable condition and $D0_{22}$ structure in the equilibrium condition. The metastable Al_3Ti despersoids have a low diffusion coefficient, which makes them thermally stable and highly resistant to coarsening. Titanium has a high solubility in the Al_3X dispersoids allowing large amounts of titanium to substitute for X in the Al_3X dispersoids, which result in improved thermal and structural stability.

[0045] Hafnium forms metastable Al_3Hf dispersoids in the aluminum matrix that have an $L1_2$ structure in the metastable condition and a $D0_{23}$ structure in the equilibrium condition. The Al_3Hf dispersoids have a low diffusion coefficient, which makes them thermally stable and highly resistant to coarsening. Hafnium has a high solubility in the Al_3X dispersoids allowing large amounts of hafnium to substitute for scandium, erbium, thulium, ytterbium, and lutetium in the above-mentioned Al_3X dispersoids, which results in stronger and more thermally stable dispersoids.

[0046] Niobium forms metastable Al_3Nb dispersoids in the aluminum matrix that have an $L1_2$ structure in the metastable condition and a $D0_{22}$ structure in the equilibrium condition. Niobium has a lower solubility in the Al_3X dispersoids than hafnium or yttrium, allowing relatively lower amounts of niobium than hafnium or yttrium to substitute for X in the Al_3X dispersoids. Nonetheless, niobium can be very effective in slowing down the coarsening kinetics of the Al_3X dispersoids because the Al_3Nb dispersoids are thermally stable. The substitution of niobium for X in the above mentioned Al_3X dispersoids results in stronger and more thermally stable dispersoids.

[0047] Al_3X $L1_2$ precipitates improve elevated temperature mechanical properties in aluminum alloys for two reasons. First, the precipitates are ordered intermetallic compounds. As a result, when the particles are sheared by glide dislocations during deformation, the dislocations separate into two partial dislocations separated by an anti-phase boundary on the glide plane. The energy to create the anti-phase boundary is the origin of the strengthening. Second, the cubic $L1_2$ crystal structure and lattice parameter of the precipitates are closely matched to the aluminum solid solution matrix. This results in a lattice coherency at the precipitate/matrix boundary that resists coarsening. The lack of an interphase boundary results in a low driving force for particle growth and resulting elevated temperature stability. Alloying elements in solid solution in the dispersed strengthening particles and in the aluminum matrix that tend to decrease the lattice mismatch between the matrix and particles will tend to increase the strengthening and elevated temperature stability of the alloy.

[0048] $L1_2$ phase strengthened aluminum alloys are important structural materials because of their excellent mechanical properties and the stability of these properties at elevated temperature due to the resistance of the coherent dispersoids in the microstructure to particle coarsening. The mechanical properties are optimized by maintaining a high volume fraction of $L1_2$ dispersoids in the microstructure. The $L1_2$ dispersoid concentration following aging scales as the amount of $L1_2$ phase forming elements in solid solution in the aluminum alloy following quenching. Examples of $L1_2$ phase forming elements include but are not limited to Sc, Er, Th, Yb, and Lu. The concentration of alloying elements in solid solution in alloys cooled from the melt is directly proportional to the cooling rate.

[0049] Exemplary aluminum alloys for this invention include, but are not limited to (in weight percent unless otherwise specified):

[0050] about Al-M-(0.1-4)Sc-(0.1-20)Gd;

[0051] about Al-M-(0.1-20)Er-(0.1-20)Gd;

[0052] about Al-M-(0.1-15)Tm-(0.1-20)Gd;
[0053] about Al-M-(0.1-25)Yb-(0.1-20)Gd;
[0054] about Al-M-(0.1-25)Lu-(0.1-20)Gd;
[0055] about Al-M-(0.1-4)Sc-(0.1-20)Y;
[0056] about Al-M-(0.1-20)Er-(0.1-20)Y;
[0057] about Al-M-(0.1-15)Tm-(0.1-20)Y;
[0058] about Al-M-(0.1-25)Yb-(0.1-20)Y;
[0059] about Al-M-(0.1-25)Lu-(0.1-20)Y;
[0060] about Al-M-(0.1-4)Sc-(0.05-4)Zr;
[0061] about Al-M-(0.1-20)Er-(0.05-4)Zr;
[0062] about Al-M-(0.1-15)Tm-(0.05-4)Zr;
[0063] about Al-M-(0.1-25)Yb-(0.05-4)Zr;
[0064] about Al-M-(0.1-25)Lu-(0.05-4)Zr;
[0065] about Al-M-(0.1-4)Sc-(0.05-10)Ti;
[0066] about Al-M-(0.1-20)Er-(0.05-10)Ti;
[0067] about Al-M-(0.1-15)Tm-(0.05-10)Ti;
[0068] about Al-M-(0.1-25)Yb-(0.05-10)Ti;
[0069] about Al-M-(0.1-25)Lu-(0.05-10)Ti;
[0070] about Al-M-(0.1-4)Sc-(0.05-10)Hf;
[0071] about Al-M-(0.1-20)Er-(0.05-10)Hf;
[0072] about Al-M-(0.1-15)Tm-(0.05-10)Hf;
[0073] about Al-M-(0.1-25)Yb-(0.05-10)Hf;
[0074] about Al-M-(0.1-25)Lu-(0.05-10)Hf;
[0075] about Al-M-(0.1-4)Sc-(0.05-5)Nb;
[0076] about Al-M-(0.1-20)Er-(0.05-5)Nb;
[0077] about Al-M-(0.1-15)Tm-(0.05-5)Nb;
[0078] about Al-M-(0.1-25)Yb-(0.05-5)Nb; and
[0079] about Al-M-(0.1-25)Lu-(0.05-5)Nb.

[0080] M is at least one of about (4-25) weight percent silicon, (1-8) weight percent magnesium, (0.1-3) weight percent manganese, (0.5-3) weight percent lithium, (0.2-6) weight percent copper, (3-12) weight percent zinc, and (1-12) weight percent nickel.

[0081] The amount of silicon present in the fine grain matrix, if any, may vary from about 4 to about 25 weight percent, more preferably from about 5 to about 20 weight percent, and even more preferably from about 6 to about 14 weight percent.

[0082] The amount of magnesium present in the fine grain matrix, if any, may vary from about 1 to about 8 weight percent, more preferably from about 3 to about 7.5 weight percent, and even more preferably from about 4 to about 6.5 weight percent.

[0083] The amount of manganese present in the fine grain matrix, if any, may vary from about 0.1 to about 3 weight percent, more preferably from about 0.2 to about 2 weight percent, and even more preferably from about 0.3 to about 1 weight percent.

[0084] The amount of lithium present in the fine grain matrix, if any, may vary from about 0.5 to about 3 weight percent, more preferably from about 1 to about 2.5 weight percent, and even more preferably from about 1 to about 2 weight percent.

[0085] The amount of copper present in the fine grain matrix, if any, may vary from about 0.2 to about 6 weight percent, more preferably from about 0.5 to about 5 weight percent, and even more preferably from about 2 to about 4.5 weight percent.

[0086] The amount of zinc present in the fine grain matrix, if any, may vary from about 3 to about 12 weight percent, more preferably from about 4 to about 10 weight percent, and even more preferably from about 5 to about 9 weight percent.

[0087] The amount of nickel present in the fine grain matrix, if any, may vary from about 1 to about 12 weight percent, more preferably from about 2 to about 10 weight percent, and even more preferably from about 4 to about 10 weight percent.

[0088] The amount of scandium present in the fine grain matrix, if any, may vary from 0.1 to about 4 weight percent, more preferably from about 0.1 to about 3 weight percent, and even more preferably from about 0.2 to about 2.5 weight percent. The Al—Sc phase diagram shown in FIG. **1** indicates a eutectic reaction at about 0.5 weight percent scandium at about 1219° F. (659° C.) resulting in a solid solution of scandium and aluminum and Al_3Sc dispersoids. Aluminum alloys with less than 0.5 weight percent scandium can be quenched from the melt to retain scandium in solid solution that may precipitate as dispersed $L1_2$ intermetallic Al_3Sc following an aging treatment. Alloys with scandium in excess of the eutectic composition (hypereutectic alloys) can only retain scandium in solid solution by rapid solidification processing (RSP) where cooling rates are in excess of about 10^{3}° C./second.

[0089] The amount of erbium present in the fine grain matrix, if any, may vary from about 0.1 to about 20 weight percent, more preferably from about 0.3 to about 15 weight percent, and even more preferably from about 0.5 to about 10 weight percent. The Al—Er phase diagram shown in FIG. **2** indicates a eutectic reaction at about 6 weight percent erbium at about 1211° F. (655° C.). Aluminum alloys with less than about 6 weight percent erbium can be quenched from the melt to retain erbium in solid solutions that may precipitate as dispersed $L1_2$ intermetallic Al_3Er following an aging treatment. Alloys with erbium in excess of the eutectic composition can only retain erbium in solid solution by rapid solidification processing (RSP) where cooling rates are in excess of about 10^{3}° C./second.

[0090] The amount of thulium present in the alloys, if any, may vary from about 0.1 to about 15 weight percent, more preferably from about 0.2 to about 10 weight percent, and even more preferably from about 0.4 to about 6 weight percent. The Al—Tm phase diagram shown in FIG. **3** indicates a eutectic reaction at about 10 weight percent thulium at about 1193° F. (645° C.). Thulium forms metastable Al_3Tm dispersoids in the aluminum matrix that have an $L1_2$ structure in the equilibrium condition. The Al_3Tm dispersoids have a low diffusion coefficient, which makes them thermally stable and highly resistant to coarsening. Aluminum alloys with less than 10 weight percent thulium can be quenched from the melt to retain thulium in solid solution that may precipitate as dispersed metastable $L1_2$ intermetallic Al_3Tm following an aging treatment. Alloys with thulium in excess of the eutectic composition can only retain Tm in solid solution by rapid solidification processing (RSP) where cooling rates are in excess of about 10^{3}° C./second.

[0091] The amount of ytterbium present in the alloys, if any, may vary from about 0.1 to about 25 weight percent, more preferably from about 0.3 to about 20 weight percent, and even more preferably from about 0.4 to about 10 weight percent. The Al—Yb phase diagram shown in FIG. **4** indicates a eutectic reaction at about 21 weight percent ytterbium at about 1157° F. (625° C.). Aluminum alloys with less than about 21 weight percent ytterbium can be quenched from the melt to retain ytterbium in solid solution that may precipitate as dispersed $L1_2$ intermetallic Al_3Yb following an aging treatment. Alloys with ytterbium in excess of the eutectic composition can only retain ytterbium in solid solution by rapid solidification processing (RSP) where cooling rates are in excess of about $10^{3\circ}$ C./second.

[0092] The amount of lutetium present in the alloys, if any, may vary from about 0.1 to about 25 weight percent, more preferably from about 0.3 to about 20 weight percent, and even more preferably from about 0.4 to about 10 weight percent. The Al—Lu phase diagram shown in FIG. **5** indicates a eutectic reaction at about 11.7 weight percent Lu at about 1202° F. (650° C.). Aluminum alloys with less than about 11.7 weight percent lutetium can be quenched from the melt to retain Lu in solid solution that may precipitate as dispersed $L1_2$ intermetallic Al_3Lu following an aging treatment. Alloys with Lu in excess of the eutectic composition can only retain Lu in solid solution by rapid solidification processing (RSP) where cooling rates are in excess of about $10^{3\circ}$ C./second.

[0093] The amount of gadolinium present in the alloys, if any, may vary from about 0.1 to about 20 weight percent, more preferably from about 0.3 to about 15 weight percent, and even more preferably from about 0.5 to about 10 weight percent.

[0094] The amount of yttrium present in the alloys, if any, may vary from about 0.1 to about 20 weight percent, more preferably from about 0.3 to about 15 weight percent, and even more preferably from about 0.5 to about 10 weight percent.

[0095] The amount of zirconium present in the alloys, if any, may vary from about 0.05 to about 4 weight percent, more preferably from about 0.1 to about 3 weight percent, and even more preferably from about 0.3 to about 2 weight percent.

[0096] The amount of titanium present in the alloys, if any, may vary from about 0.05 to about 10 weight percent, more preferably from about 0.2 to about 8 weight percent, and even more preferably from about 0.4 to about 4 weight percent.

[0097] The amount of hafnium present in the alloys, if any, may vary from about 0.05 to about 10 weight percent, more preferably from about 0.2 to about 8 weight percent, and even more preferably from about 0.4 to about 5 weight percent.

[0098] The amount of niobium present in the alloys, if any, may vary from about 0.05 to about 5 weight percent, more preferably from about 0.1 to about 3 weight percent, and even more preferably from about 0.2 to about 2 weight percent.

[0099] In order to have the best properties for the fine grain matrix, it is desirable to limit the amount of other elements. Specific elements that should be reduced or eliminated include no more than about 0.1 weight percent iron, 0.1 weight percent chromium, 0.1 weight percent vanadium, and 0.1 weight percent cobalt. The total quantity of additional elements should not exceed about 1% by weight, including the above listed impurities and other elements.

2. $L1_2$ Alloy Powder Formation and Consolidation

[0100] The highest cooling rates observed in commercially viable processes are achieved by gas atomization of molten metals to produce powder. Gas atomization is a two fluid process wherein a stream of molten metal is disintegrated by a high velocity gas stream. The end result is that the particles of molten metal eventually become spherical due to surface tension and finely solidify in powder form. Heat from the liquid droplets is transferred to the atomization gas by convection. The solidification rates, depending on the gas and the surrounding environment, can be very high and can exceed $10^{6\circ}$ C./second. Cooling rates greater than $10^{3\circ}$ C./second are typically specified to ensure supersaturation of alloying elements in gas atomized $L1_2$ aluminum alloy powder in the inventive process described herein.

[0101] A schematic of typical vertical gas atomizer **100** is shown in FIG. **6**A. FIG. **6**A is taken from R. Germain, Powder Metallurgy Science Second Edition MPIF (1994) (chapter 3, p. 101) and is included herein for reference. Vacuum or inert gas induction melter **102** is positioned at the top of free flight chamber **104**. Vacuum induction melter **102** contains melt **106** which flows by gravity or gas overpressure through nozzle **108**. A close up view of nozzle **108** is shown in FIG. **6**B. Melt **106** enters nozzle **108** and flows downward till it meets the high pressure gas stream from gas source **110** where it is transformed into a spray of droplets. The droplets eventually become spherical due to surface tension and rapidly solidify into spherical powder **112** which collects in collection chamber **114**. The gas recirculates through cyclone collector **116** which collects fine powder **118** before returning to the input gas stream. As can be seen from FIG. **6**A, the surroundings to which the melt and eventual powder are exposed are completely controlled.

[0102] There are many effective nozzle designs known in the art to produce spherical metal powder. Designs with short gas-to-melt separation distances produce finer powders. Confined nozzle designs where gas meets the molten stream at a short distance just after it leaves the atomization nozzle are preferred for the production of the inventive $L1_2$ aluminum alloy powders disclosed herein. Higher superheat temperatures cause lower melt viscosity and longer cooling times. Both result in smaller spherical particles.

[0103] A large number of processing parameters are associated with gas atomization that affect the final product. Examples include melt superheat, gas pressure, metal flow rate, gas type, and gas purity. In gas atomization, the particle size is related to the energy input to the metal. Higher gas pressures, higher superheat temperatures and lower metal flow rates result in smaller particle sizes. Higher gas pressures provide higher gas velocities for a given atomization nozzle design.

[0104] To maintain purity, inert gases are used, such as helium, argon, and nitrogen. Helium is preferred for rapid solidification because the high heat transfer coefficient of the gas leads to high quenching rates and high supersaturation of alloying elements.

[0105] Lower metal flow rates and higher gas flow ratios favor production of finer powders. The particle size of gas atomized melts typically has a log normal distribution. In the turbulent conditions existing at the gas/metal interface during atomization, ultra fine particles can form that may reenter the gas expansion zone. These solidified fine particles can be carried into the flight path of molten larger droplets resulting in agglomeration of small satellite particles on the surfaces of larger particles. An example of small satellite particles attached to inventive spherical $L1_2$ aluminum alloy powder is shown in the scanning electron microscopy (SEM) micrographs of FIGS. **7**A and **7**B at two magnifications. The spherical shape of gas atomized aluminum powder is evident. The spherical shape of the powder is suggestive of clean powder without excessive oxidation. Higher oxygen in the powder results in irregular powder shape. Spherical powder helps in improving the flowability of powder which results in higher apparent density and tap density of the powder. The satellite particles can be minimized by adjusting processing parameters to reduce or even eliminate turbulence in the gas atomization process. The microstructure of gas atomized aluminum alloy powder is predominantly cellular as shown in the optical micrographs of cross-sections of the inventive alloy in FIGS. **8**A and **8**B at two magnifications. The rapid cooling rate suppresses dendritic solidification common at slower cooling rates resulting in a finer microstructure with minimum alloy segregation.

[0106] Oxygen and hydrogen in the powder can degrade the mechanical properties of the final part. It is preferred to limit the oxygen in the $L1_2$ alloy powder to about 1 ppm to 2000 ppm. Oxygen is intentionally introduced as a component of the helium gas during atomization. An oxide coating on the $L1_2$ aluminum powder is beneficial for two reasons. First, the coating prevents agglomeration by contact sintering and secondly, the coating inhibits the chance of explosion of the powder. A controlled amount of oxygen is important in order to provide good ductility and fracture toughness in the final consolidated material. Hydrogen content in the powder is controlled by ensuring the dew point of the helium gas is low. A dew point of about minus 50° F. (minus 45.5° C.) to minus 100° F. (minus 73.3° C.) is preferred.

[0107] In preparation for final processing, the powder is classified according to size by sieving. To prepare the powder for sieving, if the powder has zero percent oxygen content, the powder may be exposed to nitrogen gas which passivates the powder surface and prevents agglomeration. Finer powder sizes result in improved mechanical properties of the end product. While minus 325 mesh (about 45 microns) powder can be used, minus 450 mesh (about 30 microns) powder is a preferred size in order to provide good mechanical properties in the end product. During the atomization process, powder is collected in collection chambers in order to prevent oxidation of the powder. Collection chambers are used at the bottom of atomization chamber **104** as well as at the bottom of cyclone collector **116**. The powder is transported and stored in the collection chambers also. Collection chambers are maintained under positive pressure with nitrogen gas which prevents oxidation of the powder.

[0108] A schematic of the $L1_2$ aluminum powder manufacturing process is shown in FIG. **9**. In the process aluminum **200** and L12 forming (and other alloying) elements **210** are melted in furnace **220** to a predetermined superheat temperature under vacuum or inert atmosphere. Preferred charge for furnace **220** is prealloyed aluminum **200** and $L1_2$ and other alloying elements before charging furnace **220**. Melt **230** is then passed through nozzle **240** where it is impacted by pressurized gas stream **250**. Gas stream **250** is an inert gas such as nitrogen, argon or helium, preferably helium. Melt **230** can flow through nozzle **240** under gravity or under pressure. Gravity flow is preferred for the inventive process disclosed herein. Preferred pressures for pressurized gas stream **250** are about 50 psi (10.35 MPa) to about 750 psi (5.17 MPa) depending on the alloy.

[0109] The atomization process creates molten droplets **260** which rapidly solidify as they travel through agglomeration chamber **270** forming spherical powder particles **280**. The molten droplets transfer heat to the atomizing gas by convention. The role of the atomizing gas is two fold: one is to disintegrate the molten metal stream into fine droplets by transferring kinetic energy from the gas to the melt stream and the other is to extract heat from the molten droplets to rapidly solidify them into spherical powder. The solidification time and cooling rate vary with droplet size. Larger droplets take longer to solidify and their resulting cooling rate is lower. On the other hand, the atomizing gas will extract heat efficiently from smaller droplets resulting in a higher cooling rate. Finer powder size is therefore preferred as higher cooling rates provide finer microstructures and higher mechanical properties in the end product. Higher cooling rates lead to finer cellular microstructures which are preferred for higher mechanical properties. Finer cellular microstructures result in finer grain sizes in consolidated product. Finer grain size provides higher yield strength of the material through the Hall-Petch strengthening model.

[0110] Key process variables for gas atomization include superheat temperature, nozzle diameter, helium content and dew point of the gas, and metal flow rate. Superheat temperatures of from about 150° F. (66° C.) to 200° F. (93° C.) are preferred. Nozzle diameters of about 0.07 in. (1.8 mm) to 0.12 in. (3.0 mm) are preferred depending on the alloy. The gas stream used herein was a helium nitrogen mixture containing 74 to 87 vol. % helium. The metal flow rate ranged from about 0.8 lb/min (0.36 kg/min) to 4.0 lb/min (1.81 kg/min). The oxygen content of the $L1_2$ aluminum alloy powders was observed to consistently decrease as a run progressed. This is suggested to be the result of the oxygen gettering capability of the aluminum powder in a closed system. The dew point of the gas was controlled to minimize hydrogen content of the powder. Dew points in the gases used in the examples ranged from −10° F. (−23° C.) to −110° F. (−79° C.).

[0111] The powder is then classified by sieving process **290** to create classified powder **300**. Sieving of powder is performed under an inert environment to minimize oxygen and hydrogen pickup from the environment. While the yield of minus 450 mesh powder is extremely high (95%), there are always larger particle sizes, flakes and ligaments that are removed by the sieving. Sieving also ensures a narrow size distribution and provides a more uniform powder size. Sieving also ensures that flaw sizes cannot be greater than minus 450 mesh which will be required for nondestructive inspection of the final product.

[0112] Processing parameters of exemplary gas atomization runs are listed in Table 1.

TABLE 1

Gas atomization parameters used for producing powder

Run	Nozzle Diameter (in)	He Content (vol %)	Gas Pressure (psi)	Dew Point (° F.)	Charge Temperature (° F.)	Average Metal Flow Rate (lbs/min)	Oxygen Content (ppm) Start	Oxygen Content (ppm) End
1	0.10	79	190	<−58	2200	2.8	340	35
2	0.10	83	192	−35	1635	0.8	772	27

TABLE 1-continued

Gas atomization parameters used for producing powder

Run	Nozzle Diameter (in)	He Content (vol %)	Gas Pressure (psi)	Dew Point (° F.)	Charge Temperature (° F.)	Average Metal Flow Rate (lbs/min)	Oxygen Content (ppm) Start	Oxygen Content (ppm) End
3	0.09	78	190	−10	2230	1.4	297	<0.01
4	0.09	85	160	−38	1845	2.2	22	4.1
5	0.10	86	207	−88	1885	3.3	286	208
6	0.09	86	207	−92	1915	2.6	145	88

[0113] The role of powder quality is extremely important to produce material with higher strength and ductility. Powder quality is determined by powder size, shape, size distribution, oxygen content, hydrogen content, and alloy chemistry. Over fifty gas atomization runs were performed to produce the inventive powder with finer powder size, finer size distribution, spherical shape, and lower oxygen and hydrogen contents. Processing parameters of some exemplary gas atomization runs are listed in Table 1. It is suggested that the observed decrease in oxygen content is attributed to oxygen gettering by the powder as the runs progressed.

[0114] Inventive $L1_2$ aluminum alloy powder was produced with over 95% yield of minus 450 mesh (30 microns) which includes powder from about 1 micron to about 30 microns. The average powder size was about 10 microns to about 15 microns. As noted above, finer powder size is preferred for higher mechanical properties. Finer powders have finer cellular microstructures. As a result, finer cell sizes lead to finer grain size by fragmentation and coalescence of cells during powder consolidation. Finer grain sizes produce higher yield strength through the Hall-Petch strengthening model where yield strength varies inversely as the square root of the grain size. It is preferred to use powder with an average particle size of 10-15 microns. Powders with a powder size less than 10-15 microns can be more challenging to handle due to the larger surface area of the powder. Powders with sizes larger than 10-15 microns will result in larger cell sizes in the consolidated product which, in turn, will lead to larger grain sizes and lower yield strengths.

[0115] Powders with narrow size distributions are preferred. Narrower powder size distributions produce product microstructures with more uniform grain size. Spherical powder was produced to provide higher apparent and tap densities which help in achieving 100% density in the consolidated product. Spherical shape is also an indication of cleaner and lower oxygen content powder. Lower oxygen and lower hydrogen contents are important in producing material with high ductility and fracture toughness. Although it is beneficial to maintain low oxygen and hydrogen content in powder to achieve good mechanical properties, lower oxygen may interfere with sieving due to self sintering. An oxygen content of about 25 ppm to about 500 ppm is preferred to provide good ductility and fracture toughness without any sieving issue. Lower hydrogen is also preferred for improving ductility and fracture toughness. It is preferred to have about 25-200 ppm of hydrogen in atomized powder by controlling the dew point in the atomization chamber. Hydrogen in the powder is further reduced by heating the powder in vacuum. Lower hydrogen in final product is preferred to achieve good ductility and fracture toughness.

[0116] A schematic of the $L1_2$ aluminum powder consolidation process is shown in FIG. **10**. The starting material is sieved and classified $L1_2$ aluminum alloy powders (step **310**). Blending (step **320**) is a preferred step in the consolidation process because it results in improved uniformity of particle size distribution. Gas atomized $L1_2$ aluminum alloy powder generally exhibits a bimodal particle size distribution and cross blending of separate powder batches tends to homogenize the particle size distribution. Blending (step **320**) is also preferred when separate metal and/or ceramic powders are added to the $L1_2$ base powder to form bimodal or trimodal consolidated alloy microstructures.

[0117] Following blending (step **320**), the powders are transferred to a can (step **330**) where the powder is vacuum degassed (step **340**) at elevated temperatures. The can (step **330**) is an aluminum container having a cylindrical, rectangular or other configuration with a central axis. Cylindrical configurations are preferred with hydraulic extrusion presses. Vacuum degassing times can range from about 0.5 hours to about 8 days. A temperature range of about 300° F. (149° C.) to about 900° F. (482° C.) is preferred. Dynamic degassing of large amounts of powder is preferred to static degassing. In dynamic degassing, the can is preferably rotated during degassing to expose all of the powder to a uniform temperature. Degassing removes oxygen and hydrogen from the powder.

[0118] Following vacuum degassing (step **340**), the vacuum line is crimped and welded shut (step **350**). The powder is then fully densified by blind die compaction or closed die forging as the process is sometimes called (step **360**). At this point the can may be removed by machining (step **380**) to form a useful billet (step **390**).

[0119] A schematic showing blind die compaction (process **400**) is shown in FIGS. **11**A and **11**B. The equipment comprises base **410**, die **420**, ram **430**, and means to apply pressure to ram **430** indicated by arrow **450**. Prior to compaction, billet **440** does not fill die cavity **460**. After compaction, billet **445** completely fills the die cavity and has taken the shape of die cavity **460**. The die cavities can have any shape provided they have a central symmetrical axis parallel to arrow **450**. Cylindrical shapes adopt well for extrusion billets. Canned $L1_2$ aluminum alloy powder preforms are easily densified due to the large capacity of modern hydraulic presses.

[0120] FIG. **12** is a perspective view of a direct extrusion process. In the process, a billet of, in this case, $L1_2$ aluminum alloy is extruded through a die having a cavity with a shape necessary to produce a cross-sectional profile of the final part. The components of extrusion process **500** are illustrated on the FIG. and comprise container **510**, container liner **520**, and ram **540** with dummy block **550**. Dummy block **550** isolates billet **530** from direct contact with ram **540** during extrusion. During extrusion, billet **530** is forced through opening (s) in die **560** by pressure on ram **540**. Ram **540** can be mechanically or hydraulically actuated. Hydraulic extrusion presses are preferred for higher pressure operation. During extrusion, die **560** is held in place against the ram pressure by die backer **570**. Other forms of extrusion are indirect extrusion, hydrostatic extrusion, lateral extrusion, and others known to those in the art.

[0121] An almost unlimited number of cross-sectional shapes of extrusions can be achieved. Extrusion **580** in FIG. **12** has a simple circular cross-section. FIG. **13** shows examples of other common shapes. FIG. **13**A is an example of how a bracket can be fabricated from an extrusion. FIG. **13**B is an example of a gear. FIG. **13**C is another exemplary shape. FIGS. **13**B and **13**C have hollow shapes and are formed by the process of hollow die extrusion. During extrusions, to produce parts with hollow cross-sections, the L1$_2$ aluminum alloy is divided during extrusion in port sections of a first (interior) hollow die into a plurality of portions, which are again joined (welded) to each other in a second (exterior) die with a welding chamber section, to form a welded portion, thereby producing a hollow section having a complicated profile.

[0122] A perspective representation of hollow die system **600** used to form a rectangular tube is shown in FIG. **14**. The die system comprises internal die **660** and external die **665**. Internal die **660** contains a plurality of inlet ports **620** and internal bearing **630**. When assembled, internal bearing **630** fits inside external bearing **635** such that there is clearance between bearing wall **640** of internal bearing **630** and bearing wall **645** of external bearing **635**. During extrusion, L1$_2$ alloy billet **610** is forced in direction of arrow **615** in a container (not shown) by a ram (not shown) such that the alloy is forced to flow through port (s) **620** such that it flows around internal bearing **630**. The metal rejoins in welding chamber **665** and flows through the gap between internal bearing **630** and external bearing **635** and is formed into rectangular hollow extrusion **670** with dimensions formed by bearing surfaces **640** and **645**. Die **660** (shown) is termed a porthole die. Other dies used to form extrusions with hollow features are spider and bridge dies and others known to those in the art.

[0123] L1$_2$ aluminum alloy parts useful for turbine and rocket engine applications can be rapidly and efficiently made by direct extrusion including brackets, cases, tubes, ducts, beams, spars. Extrusion parameters including extrusion temperature, billet soaking time, extrusion ratio and extrusion speed have significant influence on mechanical properties of L1$_2$ aluminum alloy duct. Billet soaking time was kept constant at 1.5 hours for all these billets. These billets were compacted at 750F using vacuum hot pressing resulting in 100% dense billets which were extruded to produce ducts. Lower extrusion temperature of 500F at ratio of 10:1 and speed of 3 inch per minute resulted in 118 ksi tensile strength, 8% elongation and 16% reduction in area. Higher extrusion temperature of 700F at ratio of 10:1 and speed of 0.5 inch per minute resulted in 115 ksi tensile strength, 9% elongation and 18.5% reduction in area. In other example, extrusion temperature of 650F at ratio of 6:1 and speed of 0.5 inch per minute resulted in 117 ksi tensile strength, about 7.5% elongation and 15% reduction in area. In other example, extrusion temperature of 700F, ratio of 15:1 and speed of 3:1 resulted in 105 ksi tensile strength, 10% elongation and 20% reduction in area. A number of examples of extrusion demonstrated excellent tensile properties with about 105-120 ksi tensile strength and ductility in terms of reduction in area of about 10 to 20%. These examples suggest that a unique combination of extrusion parameters that have been developed in the present invention can lead to a good combination of tensile strength and ductility for L1$_2$ aluminum alloys ducts and that can be applied to other extruded products also including brackets, cases, tubes, beams, spars.

[0124] Extrusions when carried at very high speeds can result in reduced strength and higher ductility due to adiabatic heating generated during extrusion. Higher the speed larger the adiabatic heat generated due to friction during extrusion. Therefore higher speed is not preferred from strength point of view. Higher speed is preferred from cost point of view since more number of components can be produced in same amount of time. Slower speeds do not produce adiabatic heat and therefore preferred for higher strength extrusions. Slower the speed less adiabatic heat is produced. However, below certain speed extrusion becomes uneconomical and therefore it is not preferred to use too low extrusion speed. Based on all the results produced, extrusion speed of about 0.1 inch per minute to about 20 inch per minute is preferred for present inventive L1$_2$ aluminum alloys based on balanced mechanical properties resulting in good combination of strength and ductility.

TABLE 2

Effect of compaction and extrusion parameters on extruded L1$_2$Al alloys duct

Billet ID	Compaction Temperature, F.	Extrusion Temperature, F.	Extrusion Ratio	Extrusion Speed, ipm	Ultimate Tensile Strength, ksi	0.2% Yield Strength, ksi	Elongation, %	Reduction in Area, %
1	750	700	10:01	0.5	115.0	104.0	9.0	18.5
2	750	650	10:01	0.5	114.0	103.0	6.5	12.0
3	750	650	6:01	0.5	117.0	107.0	7.5	15.0
4	750	600	10:01	3	112.0	10.4.0	6.5	12.5
5	750	700	15:01	3	105.0	96.0	10.0	20.0
6	750	550	10:01	3	112.0	102.0	7.5	12.0
7	750	500	10:01	3	118.0	108.0	8.0	16.0

[0125] A photograph of a duct produced for a jet engine is shown in FIG. **15**. Products such as this are a significant improvement in the industry.

[0126] Although the present invention has been described with reference to preferred embodiments, workers skilled in the art will recognize that changes may be made in form and detail without departing from the spirit and scope of the invention.

1. A method for forming a high strength aluminum alloy component containing $L1_2$ dispersoids, comprising the steps of:

- placing in a container a quantity of an aluminum alloy powder containing an $L1_2$ dispersoid $L1_2$ comprising Al_3X dispersoids wherein X is at least one first element selected from the group comprising:
  - about 0.1 to about 4.0 weight percent scandium, about 0.1 to about 20.0 weight percent erbium, about 0.1 to about 15.0 weight percent thulium, about 0.1 to about 25.0 weight percent ytterbium, and about 0.1 to about 25.0 weight percent lutetium;
  - at least one second element selected from the group comprising about 0.1 to about 20.0 weight percent gadolinium, about 0.1 to about 20.0 weight percent yttrium, about 0.05 to about 4.0 weight percent zirconium, about 0.05 to about 10.0 weight percent titanium, about 0.05 to about 10.0 weight percent hafnium, and about 0.05 to about 5.0 weight percent niobium; and
  - the balance substantially aluminum;
- the alloy powder having a mesh size of less than 450 mesh in a container,
- vacuum degassing the powder at a temperature of about 300° F. (149° C.) to about 900° F. (482° C.) for about 0.5 hours to about 8 days;
- sealing the degassed powder in the container under vacuum;
- heating the sealed container at about 300° F. (149° C.) to about 900° F. (482° C.) for about 15 minutes to eight hours;
- vacuum hot pressing the heated container to form a billet;
- removing the container from the formed billet; and
- extruding the billet into a component using an extrusion die shaped to form the component.

2. The method of claim **1**, wherein the aluminum alloy powder contains at least one ceramic selected from the group comprising: about 5 to about 40 volume percent aluminum oxide, about 5 to about 40 volume percent silicon carbide, about 5 to about 40 volume percent aluminum nitride, about 5 to about 40 volume percent titanium diboride, about 5 to about 40 volume percent titanium boride, about 5 to about 40 volume percent boron carbide and about 5 to about 40 volume percent titanium carbide.

3. The method of claim **1**, wherein the aluminum alloy powder contains at least one third element selected from the group consisting of silicon, magnesium, manganese, lithium, copper, zinc, and nickel.

4. The method of claim **3**, wherein the third element comprises at least one of about 4 to about 25 weight percent silicon, about 1 to about 8 weight percent magnesium, about 0.1 to about 3 weight percent manganese, about 0.5 to about 3 weight percent lithium, about 0.2 to about 6 weight percent copper, about 3 to about 12 weight percent zinc, about 1 to about 12 weight percent nickel.

5. The method of claim **1**, wherein the extrusion is carried out at a temperature of from about 300° F. (148.9° C.) to about 900° F. (482.2° C.).

6. The method of claim **1**, wherein the extrusion is carried out at rate of about 0.1 inch per minute to about 20 inch per minute.

7. The method of claim **1**, the billet temperature ranges from about 300° F. (148.9° C.) to about 900° F. (482.2° C.).

8. The method of claim **1**, wherein billet has a soak time ranging from about 0.5 hours to about 8 hours.

9. The method of claim **1**, wherein the extrusion is carried out at ratios of about 2:1 to 40:1.

10. The method of claim **1**, wherein the extrusion die temperature ranges from about 300° F. (148.9° C.) to about 900° F. (482.2° C.).

11. The method of claim **1**, wherein consolidating the powders comprises:

- sieving the powders to achieve a particle size of less than about −325 mesh;
- placing the powders in a container with a rectangular cross-section;
- vacuum degassing the powder;
- sealing the container; and
- hot pressing the container to achieve a powder density of about 100 percent.

12. The method of claim **1**, wherein the high strength aluminum alloy component is selected from brackets, cases, tubes, ducts, beams, spars and other components for gas turbine engines, rocket engines and other aerospace applications.

* * * * *